

Exploring E, NS3, and NS5 proteins to design a novel multi-epitope vaccine candidate against West Nile Virus: An in-silico approach

Md Wasim Alom^{*}, Mobasshir Noor Shehab, Khaled Mahmud Sujon, Farzana Akter

Department of Genetic Engineering and Biotechnology, University of Rajshahi, Rajshahi, 6205, Bangladesh



ARTICLE INFO

Keywords:

West Nile Virus
Multi-epitope vaccine
Immunoinformatics
B-cell epitopes
T-cell epitopes
In-silico

ABSTRACT

West Nile Virus is a spherical, enveloped capsid with a single-stranded RNA molecule and a known pathogen responsible for encephalitis. The deficiency of adequate treatment for WNV resulted in an increased mortality rate in its endemic zones, consequently causing its emergence as a primary health concern on both national and international scales as brain inflammation/infections caused by WNV are proved to be lethal. Thus, potential vaccination against WNV is the most viable candidate for remediation. A multi-epitope prophylactic/therapeutic vaccine targeting the pathogen's major structural and functional infective proteins (E, NS3, and NS5 proteins in this study) would be invaluable to achieve the current elimination goal. The present study was conducted with the directive to design a chimeric epitope-based vaccine exploiting immunoinformatics methods. After a thorough investigation, a plausible candidate was selected with the combination of twelve T-cell epitopes and nine B-cell epitopes along with appropriate adjuvant and linkers. Physicochemical features were analyzed, and the tertiary structure of the vaccine candidate was predicted, refined, and validated. Further molecular docking study revealed significant results of solid binding interactions of the vaccine with its specific receptor. The molecular dynamics results showed the complex rigidity, a low deformation index, and stable binding between the vaccine and the receptor with small atomic fluctuations, thus considering the vaccine as a potential candidate. Furthermore, an immune simulation was also performed to observe the immunological responses upon administration into humans, which evaluate the efficiency of the vaccine construct to derive robust immune responses like increased level of T-cells, cytokines, and antibodies to combat against the virus. Finally, codon adaptation and in-silico cloning were accomplished to design an effective mass production strategy of the vaccine. This study implies that the predicted vaccine can be a potential candidate that must undergo wet-lab-based observations.

1. Introduction

West Nile virus (WNV) is a zoonotic arthropod-borne virus belonging to the Flaviviridae family and one of the primary causative agents for encephalitis pathogenesis; a member of the Japanese encephalitis virus serocomplex [1]. WNV was first detected and identified in the West Nile province of Uganda in December 1937 from a female African individual [2]. Infrequent mild febrile illnesses caused by WNV were observed in Israel from the 1950s [3]. After almost five decades, the prevalence of WNV was noticed in the northeastern United States [4]. Since then, the

appearance of the virus has been widely distributed across Canada, the United States, Mexico [5], Algeria, Egypt, Greece, Morocco, Romania, Tunisia, Russia, France, Italy, and many other countries [6]. Moreover, WNV was declared an endemic virus in the USA in 2002 [7].

West Nile Virus is an arbovirus that prevailed in nature by an enzootic transmission cycle between many avian and mosquito species. Mosquitoes are the preferred vectors, whereas birds act as the natural reservoir hosts of transmission. Initially, WNV is transmitted by *Culex* sp. Mosquito's other genera, including *Aedes*, *Anopheles* in the presence of favorable circumstances [8]. WNV has already been identified and

Abbreviations: WNV, West Nile Virus; MHC, major histocompatibility complex; CTL, Cytotoxic T-lymphocyte; HTL, Helper T-lymphocyte; ORF, Open Reading Frame; CD4, cluster of differentiation 4; CD8, cluster of differentiation 8; BLAST, Basic Local Alignment Search Tool; IFN, Interferon; IL, Interleukin; 2D, two dimensional; 3D, three dimensional; E, Envelope; HLA, human leukocyte antigen; *E. coli*, *Escherichia coli*; NS, non-structural; AAY, Ala-Ala-Tyr; KK, Lys-Lys; GPGPG, Gly-Pro-Gly-Pro-Gly; GGGS, Gly-Gly-Gly-Ser; EAAAK, Glu-Ala-Ala-Ala-Lys; TLR4, toll-like receptor 4; WHO, World Health Organization.

* Corresponding author.

E-mail address: wasimalom22@gmail.com (M.W. Alom).

<https://doi.org/10.1016/j imu.2021.100644>

Received 15 March 2021; Received in revised form 16 June 2021; Accepted 16 June 2021

Available online 19 June 2021

2352-9148/© 2021 The Authors

Published by Elsevier Ltd.

This is an open access article under the CC BY-NC-ND license

(<http://creativecommons.org/licenses/by-nd/4.0/>).

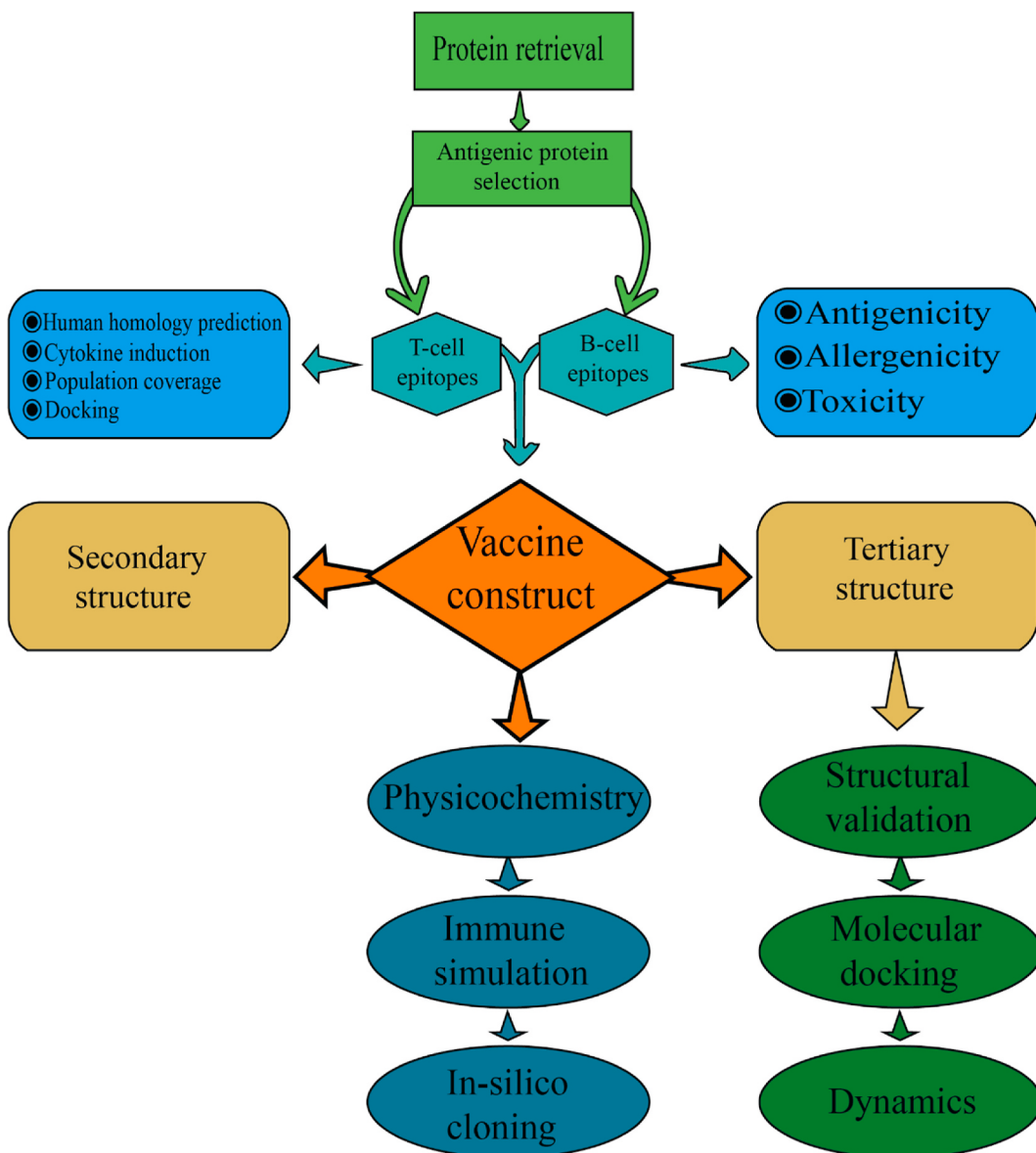


Fig. 1. Schematic representation of the overall workflow applied in the current study. The entire approach used in the study comprises of various phases, which involves protein retrieval and antigenic protein selection. Epitope predictions from the chosen protein (CTL, HTL and B-cell epitopes); vaccine construction and its physicochemical quality check. Molecular docking of the vaccine with immune cell receptor, followed by molecular dynamics to check binding stability. Finally codon adaptation and immune simulation to understand immune responses.

isolated from over 40 species of mosquitoes, mainly in the *Culex* genus [9]. Besides, the natural reservoir for WNV is house sparrows, crows, magpies, jays, house finches, and grackles which are predominantly infected by mosquitoes and develop high levels of viremia. The redundancy of WNV transmission is discerned primarily by the outbreak and a plethora of compatible vectors [10]. Humans and several mammals, particularly horses, are considered incidental hosts with a low level of viremia and do not contribute to the viral transmission cycle [11].

WNV isolates identified from various countries have been categorized into two genetic lineages (I and II) mainly based on substitutions of the amino acid residue in their envelope protein [12]. Comparatively, Lineage I have been responsible for outbreaks and severe human disease [6]. The WNV structure was explicated by utilizing cryo-electron microscopy (cryo-EM) and image reconstruction techniques. The virus has icosahedral symmetry surrounded by a lipid bilayer with a diameter of 500 Å devoid of spikes or projections [13]. WNV genome consists of an enveloped single-stranded positive-sense RNA molecule that can be considered as a virion. Genome sequence analysis indicates

approximately 11,000 nucleotides in length with an open reading frame (ORF) [14]. Generally, the virion is composed of a membrane envelope derived from the host and a nucleocapsid containing the viral genome (RNA) surrounded by the envelope [15]. The viral RNA encodes a single polyprotein to produce three structural and seven non-structural (NS) proteins [16]. The resulting three viral structural proteins are capsid, pre-membrane/membrane, and envelope protein [17], while NS1, NS2A, NS2B, NS3, NS4A, NS4B, and NS5 are the seven non-structural proteins [18–20]. The 5' end of the ORF encodes the structural proteins; on the other hand 3' end of the ORF encodes the non-structural proteins [21,22]. The structural proteins are responsible for the viral fusion with the host cell membrane, viral entry, and genomic assembly [23–25]. In addition, the non-structural proteins serve as co-factor and makeup materials and types of machinery for intracellular viral replication [26–28].

The West Nile Virus associated diseases can be mild and severe. The WNV can cause febrile illness (West Nile Fever), neuro-invasive disease such as encephalitis, meningoencephalitis, meningitis, or poliomyelitis-

like acute flaccid paralysis (AFP), and also non-neuro-invasive disease [11,29–31]. Usually majority of the patients, approximately 80% of WNV infections, are asymptomatic, and the rest, 20% leading to West Nile fever or other severe neuro-invasive diseases [32]. During 1999–2018, total cases of 50,830 patients to be infected, and 2330 deaths were reported in the United States [33]. Over the last two decades, the alarming prevalence of WNV has spread throughout the globe. Still, no specific antivirus, vaccine, or post-exposure therapy for WNV is currently available. Therefore, identifying the drug treatment options is of extreme necessity as soon as possible to secure public health. In this situation, bioinformatics-aided vaccine design can be a potential approach for the prevention of WNV. Our study was aimed to design a multi-epitope vaccine through immunoinformatics to stimulate an immune response against WNV.

Immune responses play one of the critical roles in fighting viral infections [34]. Conventional vaccines consist of entire organisms or large proteins, thus incorporating unwanted antigens, leading to increased allergenic reactions [35]. These limitations can be defeated by using multi-epitope vaccines, thereby abstaining from the possibility of allergenic reaction [36–38]. A multi-epitope vaccine comprises a series of immunogenic peptide fragments that can activate adaptive immune responses [39,40]. Compared with conventional or single-epitope vaccines, multi-epitope vaccines have identical features: they consist of multiple MHC restricted CTL, HTL and B-cell epitopes that could induce potential cellular and humoral immune responses simultaneously exacerbate the capacity of immunization and abate unnecessary components responsible for adverse effects [34]. The multi-epitope vaccines designed by the immunoinformatics approach also save time and cost and raise the feasibility of effective vaccine design [35]. This immunoinformatics technique has been utilized to design multi-epitope vaccines against Hepatitis [41], Dengue [42], Ebola [43], Respiratory Syncytial Virus [44], Lassa virus [45], Zika virus [46], and many more. Therefore, designing a multi-epitope vaccine is an ideal approach for prophylactic measures of viral infections.

In this study, we have thoroughly exploited several computational tools to identify immunogenic B and T-cell epitopes via the means of reverse vaccinology for vaccine development. It provides simple, reliable, and efficient methods to identify the appropriate B and T-cell epitopes [47]. Afterward, a vaccine candidate was designed using the most suited epitopes along with adjuvant and linkers. We considered a TLR4 agonist adjuvant which is required for optimal translation and maximal rate of vaccine synthesis. Therefore, 50 S ribosomal protein L7/L12 was used as the adjuvant, which helps recruit dendritic cells and T-cells to potentiate antigen-specific immune responses [48]. The protein sequence of the constructed vaccine was used for analyzing physicochemical features and immunogenic profiling, succeeded by the secondary structural features and 3D model prediction. The tertiary structure in consideration was subjected to refinement and validation.

Moreover, disulfide bonds were generated to enhance structural durability. Molecular docking was conducted by an automated tool to quantify binding mode and interactions between the vaccine and the receptor. Molecular docking is a computational approach to explore the binding affinity with a protein [49]; therefore, it is a key tool in structural molecular biology and computer-aided drug or vaccine design [50]. It has a vast application area, including peptide interaction, drug interaction, virtual screening on large library, lead optimization, binding studies, and combinatorial library design [51]. A molecular dynamics study was also performed using an online server to strengthen the prediction. Molecular dynamics is a simulation methodology for investigating the physical movements of atoms and their binding stability by using Newton's equation of motion [52]. It has become a vital technique that can be used to explore the conformational space of proteins, to study dynamic properties of the proteins, to explore ligand-protein complex binding stability, protein fold structures, and prediction of an ensemble of structures for a protein in its native state [52–54].

Consequently, an immune simulation was rendered to mimic and therefore estimate the immunogenic response in actual life. Finally, we proceeded with Codon adaptation and in silico cloning to investigate the expression of vaccine protein within the suitable host. A flow chart representing the procedure mentioned above in its entirety, from the antigen selection to vaccine construction and evaluation, is illustrated in Fig. 1.

2. Materials and methods

2.1. Retrieval of viral protein sequences

The National Center for Biotechnology Information (NCBI) at www.ncbi.nlm.nih.gov was exploited for retrieving target proteins. In addition, the amino acids sequence of envelope protein E (accession: NP_776,014), capsid protein C (accession: NP_776,010), non-structural protein NS1 (accession: NP_776,015), non-structural protein NS3 (accession: NP_776,018), and nonstructural protein NS5 (accession: NP_776,022) of West Nile Virus were retrieved in FASTA format and were subjected to further analysis. The most immunologically significant protein of WNV is E-glycoprotein, which directly involves in virus-host interaction and viral genome release [55]. The capsid protein is associated with the viral genome and viral assembly, where NS proteins serve as appliances for viral replication [56]. The viral glycoprotein NS1 serves as an essential co-factor for viral replication and antagonist of TLR signaling [57]. The NS3 proteins encode viral proteases, and NS5 encodes RNA-dependent RNA polymerase for viral replication [58,59]. Due to the involvement in pathogenesis, we selected these proteins as mentioned above for vaccine design.

2.2. Antigenicity and physicochemical properties analysis of the target protein sequences

The VaxiJen v2.0 server (<http://www.ddg-pharmfac.net/vaxijen/VaxiJen/VaxiJen.html>) was used for analyzing the antigenicity of protein sequences using 0.4 as the threshold [60]. VaxiJen is a sequence alignment-independent bioinformatics tool for predicting potent antigens within a pathogen [61,62]. Further, the target proteins were predicted using the ExPasy ProtParam tool (<https://web.expasy.org/protparam/>) to analyze physicochemical properties, including the molecular weight, theoretical pI, composition of amino acid, grand average of hydropathicity (GRAVY), instability index [63].

2.3. T-cell and B-cell epitope prediction

T-cells are one of the significant components of adaptive immunity that focuses on specific foreign particles [64]. Cytotoxic T-lymphocytes are specialized for, killing infected cells directly [65]. Helper T-lymphocytes recognize foreign antigens and activate B-cells and cytotoxic T-cells to destroy infected target cells [66]. B-cells also represent a major part of humoral immunity. Unlike T-cells, they don't destroy viruses directly but helps in adaptive immunity by secreting antibodies [67]. So, the T cell and B cell epitopes for selected proteins were predicted using the freely accessible online server IEDB or Immune Epitope Database (<https://www.iedb.org/>). The MHC class-I restricted CD8⁺ cytotoxic T-lymphocyte (CTL) epitopes were identified by NetMHCpan EL 4.0 prediction method [68] for HLA-A*01-01 and HLA-A*02-01 alleles as well MHC class-II restricted CD4⁺ helper T-lymphocyte (HTL) epitopes were obtained using IEDB recommended consensus 2.22 prediction method [69] for HLA DRB1*01-01 allele. Next, B-cell epitopes were predicted predominantly with an amino acid number greater than twelve using the BepiPred linear epitope prediction 2.0 method [70].

2.4. Antigenicity, allergenicity, and toxicity analysis of the epitopes

The antigenicity of the epitopes was identified using the VaxiJen

v2.0 server (<http://www.ddg-pharmfac.net/vaxijen/VaxiJen/VaxiJen.html>) keeping threshold 0.4 to resolve the accuracy of the prediction. The online server AllerTOP v.2.0 (<https://www.ddg-pharmfac.net/AllerTOP/>) was utilized to generate allergenicity. AllerTOP is the alignment-independent online tool for allergenicity prediction, generating precise results [71]. In addition, the toxicity prediction was conducted using ToxinPred (<http://crdd.osdd.net/raghava/toxinpred/>) utilizing an SVM (support vector method) based method with default parameters [72].

2.5. Human homology prediction and cytokine induction capacity analysis of the epitopes

The homology prediction of the epitopes with *Homo sapiens* was carried out by using the Protein BLAST(BLASTp) tool (<https://blast.ncbi.nlm.nih.gov/Blast.cgi>) where the E values exceeding the score of 0.05 were considered as the non-homologous epitopes. Additionally, the cytokine induction capacity was predicted for MHC class-II epitopes only because they induce cytokine release. IFN-gamma induction of the MHC class-II epitopes was identified using an online tool IFNepitope (<http://crdd.osdd.net/raghava/ifnepitope/design.php>) [73]. Similarly, IL-4 inducing capacity was predicted utilizing the IL4pred tool (<http://crdd.osdd.net/raghava/il4pred/index.php>) [74].

2.6. Population coverage analysis

A vaccine molecule must share broad-spectrum protection against the various population to accumulate maximum efficiency. Besides, HLA alleles are highly polymorphic, meaning that their distribution norm varies among different geographic areas and ethnic groups around the globe. Therefore, T-cell epitopes and their respective HLA binding alleles, were used to calculate population coverage using the IEDB population coverage tool (<http://tools.iedb.org/population/>) [75].

2.7. Peptide modeling and molecular docking

After different bioinformatics investigations, only the superior epitopes were selected for the Peptides and HLAs interaction pattern analysis. The Three-Dimensional (3D) structures of the selected T-cell epitopes were generated utilizing Peptide Structure Prediction server PEP-FOLD3 (<https://mobyle.rpbs.univ-paris-diderot.fr/cgi-bin/portal.py#forms:PEP-FOLD3>) [76]. Through analysis of the epitope-wise HLA binding alleles, HLA-A*01:01 (PDB ID: 4NQV) and HLA-A*02:01 (PDB ID: 3MGO) were selected for MHC class-I epitopes, whereas HLA-DRB1*01:01 (PDB ID: 1AQD) was considered for MHC class-II epitopes. The crystalline structures of the three binding HLA alleles were retrieved from Protein Data Bank (PDB) (<https://www.rcsb.org/>) [77] and processed with PyMOL [78]. Ultimately, the molecular docking of the epitopes with their respective HLA binding alleles was conducted using an online PatchDock server (<https://bioinfo3d.cs.tau.ac.il/PatchDock/php.php>). PatchDock uses a specific docking algorithm to detect a transformation of one of the molecules and interaction between them without causing a steric clash where the server discerns the best candidates based on RMSD scores [79]. The refinement and re-scoring were carried out through the FireDock server (<http://bioinfo3d.cs.tau.ac.il/FireDock/>) [80]. The docking interactions were visualized using BIOVIA Discovery Studio 2019 [81].

2.8. Designing of final vaccine construct

A plausible epitope-based vaccine was constructed against West Nile Virus. The T-cell epitopes, B-cell epitopes, and a suitable adjuvant were included and joined together by different flexible linkers for the vaccine construction. The AAY, GPGPG, and KK linkers were used to conjugate the epitopes. The utilized linkers confirmed the separation of the individual epitopes. The AAY (Ala-Ala-Tyr) linker, which is a type of

cleavage site of proteasomes, was used to augment epitope presentation and enhances protein stability [82,83]. The AAY and GPGPG, known as glycine-proline linkers, prevent junctional epitopes [84,85]. The KK or bi-lysine linker facilitates the immunogenic activity of the vaccine construct. The TLR4 agonist 50 S ribosomal protein L7/L12 was included as an effective adjuvant to enhance the immunogenicity of the vaccine protein [48]. The adjuvant was linked to the vaccine sequence through the EAAAK linker, which enhances the immunogenicity of the vaccine construct [86].

2.9. Prediction of antigenicity, allergenicity, and various physicochemical properties of the formulated vaccine

The antigenicity of the final vaccine candidate was analyzed by the VaxiJen v2.0 tool (<http://www.ddg-pharmfac.net/vaxijen/VaxiJen/VaxiJen.html>), and the prediction threshold was kept at 0.4. The non-allergic behavior was predicted using AllerTOP v.2.0 server (<https://www.ddg-pharmfac.net/AllerTOP/>). Later, the ProtParam server (<https://web.expasy.org/protparam/>) was utilized for the various physicochemical features of the constructed vaccine such as Molecular weight, Theoretical pI, Ext. Coefficient (in M⁻¹ cm⁻¹), Instability index, Aliphatic index, Grand average of hydropathicity (GRAVY).

2.10. Secondary and tertiary structure prediction of the vaccine candidate

The secondary structural properties of the final vaccine protein were determined using the PSIPRED v4.0 (PSI-blast based secondary structure prediction) server (<http://bioinf.cs.ucl.ac.uk/psipred/>) [87] and SIMPA96 secondary structure prediction method at (https://npsa-prabi.ibcp.fr/cgi-bin/npsa_automat.pl?page=/NPSA/npsa_simpa96.html) [88]. Then secondary structural properties, including alpha-helix, beta-sheet, random coils, were retrieved and analyzed for the structural quality of the vaccine candidate. The vaccine's three-dimensional (3D) model was prepared using the GalaxyWEB server (<http://galaxy.seoklab.org/>). GalaxyWEB is a web server for tertiary structure prediction and refinement by template-based modeling [89].

2.11. Vaccine tertiary structure refinement and validation

The tertiary structure refinement is the quality improvement process which is a vital step for vaccine design. The retrieved 3D structure of the vaccine was refined using the GalaxyRefine (<http://galaxy.seoklab.org/refine>) web-based server. This server provided a robust and overall ranking, performed by a CASP10 based refinement technique [90]. The refined structure was visualized using BIOVIA Discovery Studio 2019 [81]. Further, the Ramachandran plot assessment of the purified protein structure was conducted using RAMPAGE (<http://mordred.bioc.cam.ac.uk/~rapper/rampage2.php>) server to analyze its overall quality [91].

2.12. Vaccine protein disulfide engineering

Disulfide bonds in proteins are formed between two cysteine residues of individual chains, which provide stability of their folded state. Therefore, protein disulfide engineering was conducted with the help of the Disulfide by Design 2 (DbD2) server (<http://cptweb.cpt.wayne.edu/DbD2/>) to predict disulfide bonds and their respective positions in vaccine protein [92].

2.13. Molecular docking of the vaccine with receptor

Protein-protein docking is a widely used computer simulation approach that aims to assess the conformation and interaction mode of a receptor-ligand complex. The PDB file of TLR-4 (PDB ID: 4G8A) was retrieved from RCSB Protein Data Bank (PDB) (<https://www.rcsb.org/>),

Table 1

The selected MHC class-I epitopes for the final vaccine construction.

Epitope	Antigenicity	AS	Allergenicity	Toxicity	Human homology
YVGKTVWFV	Antigen	0.85	Non-allergen	Non-toxic	Non-homologous
KGDTTGVY	Antigen	0.44	Non-allergen	Non-toxic	Non-homologous
KTVWFVPSV	Antigen	0.86	Non-allergen	Non-toxic	Non-homologous
MSPHRVPNY	Antigen	0.42	Non-allergen	Non-toxic	Non-homologous
FMWLGARF	Antigen	1.311	Non-allergen	Non-toxic	Non-homologous
FLAVGGVLL	Antigen	0.79	Non-allergen	Non-toxic	Non-homologous
VLLFLSVNV	Antigen	0.50	Non-allergen	Non-toxic	Non-homologous
GMSWITQGL	Antigen	0.87	Non-allergen	Non-toxic	Non-homologous
GTVVLELQY	Antigen	1.51	Non-allergen	Non-toxic	Non-homologous
SVGEKSFLV	Antigen	0.71	Non-allergen	Non-toxic	Non-homologous

which is considered as the receptor molecule while vaccine protein as ligand. The removal of water processed the receptor protein and other unnecessary molecules, succeeded by the separation of attached ligand in the receptor. These processes were executed by PyMOL [78] molecular graphics system (<https://www.pymol.org/>). In order to predict the binding pattern, the PDB file of vaccine protein and TLR-4 was submitted into ClusPro 2.0 (<https://cluspro.bu.edu/login.php>) server [93]. The ClusPro 2.0 server works conducting PIPER, a Fast Fourier transform (FFT) based docking program which performs three computational steps as follows: (1) rigid-body docking (2) generation of 1000 lowest energy structures based on RMSD (3) energy minimization to remove steric clashes. This server generates results based on their lowest energy scores and center scores [94]. The binding affinity of the docked complex was determined by the PRODIGY tool of the HADDOCK server (<https://bianca.science.uu.nl/prodigy/>) [95]. The lower score generated by the PRODIGY tool exhibits a higher binding affinity [96]. The docked complex was visualized by BIOVIA Discovery Studio 2019 [81].

2.14. Molecular dynamics simulation

After performing the protein-protein docking study, the docked complex was subjected to molecular structure dynamics simulation to determine the stability in the ligand-receptor complex interaction for strengthening the prediction. The high-performance molecular dynamics simulation was conducted by the Internal coordinates normal mode analysis server iMODS (<http://imods.chaconlab.org>) [97]. This is a frequently used and versatile online server that explained the collective functional motions of protein through normal mode analysis (NMA) and provides B-factors, eigenvalues, deformability, elastic network, variance, and co-variance map [98]. Deformation index of a complex delineates the stable binding capacity and efficiency of the ligand to the receptor molecule with a few atomic fluctuations [99]. The Eigen score also demonstrates binding stability, where a low score implies less stability and easy deformation of the atoms in the molecules [100].

2.15. In silico evaluation of immune response

To estimate the feasible immune response of the final vaccine, immune simulation was performed utilizing the C-IMMSIM v10.1 server (<http://www.cbs.dtu.dk/services/C-ImmSim-10.1/>). For instance, the minimum interval period was four weeks between dose 1 and 2. All parameters were kept default, and three injections were given with time steps of 1, 84, and 168 respectively, where each time step is equal to 8 h. This immune simulator performs on a position-specific scoring matrix (PSSM) to predict immune responses [101].

2.16. Codon optimization and in silico cloning

The constructed vaccine was reverse transcribed to a probable DNA sequence for inducing the expression rate within a characterized host organism. Hence, the protein sequence of the vaccine was submitted into

Java Codon Adaptation Tool (JCat) (<http://www.jcat.de/>) server for the codon optimization [102]. Herein, we selected *E. coli* (strain k12) as the host organism and avoided the following three criteria; rho-independent transcription terminators, binding sites of the prokaryotic ribosome, and cleavage site of EcoR1 and Xho1 restriction enzymes [103,104]. Then the adapted DNA sequence of the vaccine protein was taken, and restriction sites of EcoR1 and Xho1 were added to the N-terminal and C-terminal, respectively. Finally, the adapted DNA sequence was inserted into the pET28a (+) expression vector between EcoR1 and Xho1 restriction sites. This in-silico process was carried out through SnapGene v4.2 software (<https://www.snapgene.com/>) [105].

3. Results

3.1. Selection of antigenic protein

A total of five proteins were retrieved from the NCBI database and undergone immunogenic prediction and physicochemical features analysis (Supplementary table 1). Following the investigation, we selected envelope protein E (antigenic score: 0.72), non-structural protein NS3 (antigenic score: 0.48) and non-structural protein NS5 (antigenic score: 0.42) for epitope prediction.

3.2. Potential T-cell epitope prediction

The IEDB server generated a good number of epitopes for all three selected proteins severally. According to their antigenicity scores and percentile scores, we picked the best fifteen MHC class-I (Supplementary table 2, 5, 8) and fifteen MHC class-II epitopes (Supplementary table 3, 6, 9) of individual proteins for assessment. Then, antigenicity, allergenicity, toxicity, and human homology prediction were carried out for all the epitopes. After the assessment, ten best MHC class-I epitopes were selected for vaccine construction (Table 1). In addition, two MHC class-II epitopes which have cytokine induction capacity were chosen for final vaccine construction (Table 2).

3.3. Potential B-cell epitope prediction

The IEDB server predicted the B-cell epitopes. We picked the best five epitopes for E protein and ten for NS3 and NS5 separately for evaluation (Fig. 2) (Supplementary table 4, 7, 10). After the evaluation, nine B-cell epitopes of three proteins were antigenic, non-toxic, and non-allergenic (Table 3). All these nine epitopes were selected for vaccine design purposes.

3.4. Worldwide population coverage analysis

The selected MHC class-I and MHC class-II epitopes used for vaccine construction and their respective HLA binding alleles, were obtained to assess worldwide population coverage. Both the MHC class-I and MHC class-II epitopes provided a high percentage of population coverage throughout the world (Supplementary table 11). The selected epitopes exhibited interactions with various other HLA alleles from different countries such as Bulgaria (78.93%), England (78.88%), Ireland South (78.03%), and more (Fig. 3). This analysis suggests that the designed vaccine could be an efficient candidate for most of the population across the world.

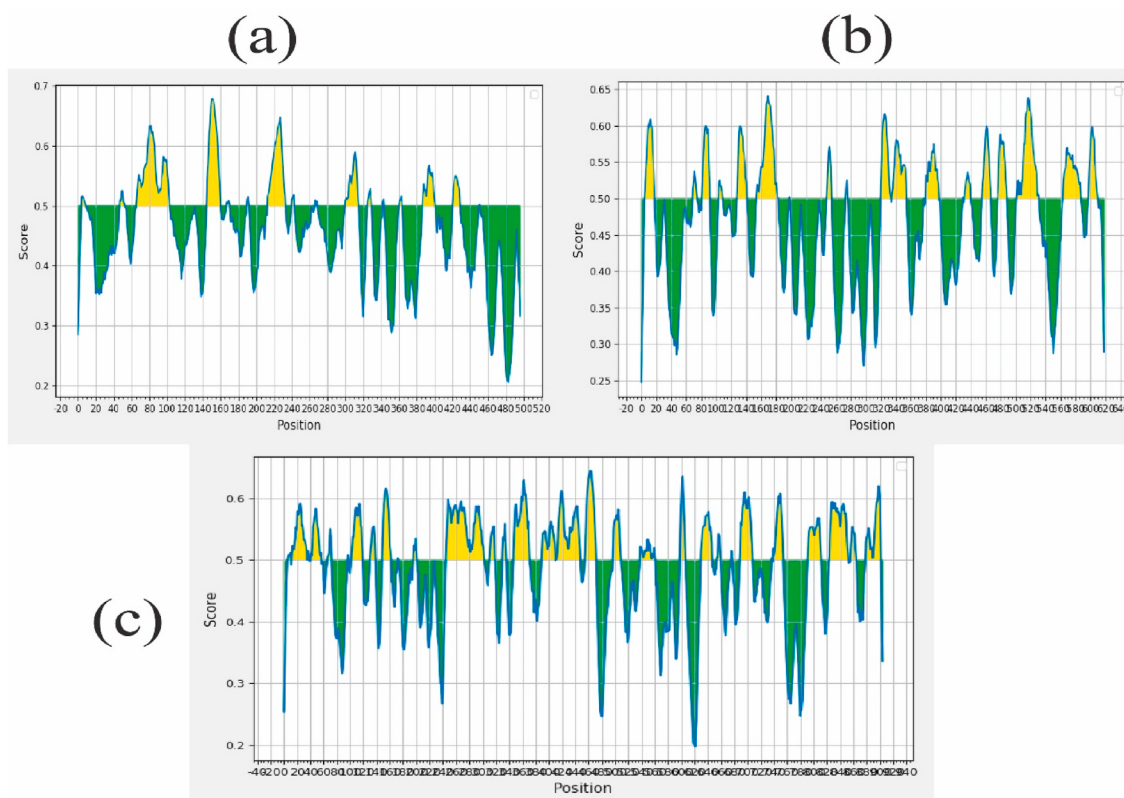
3.5. Molecular docking analysis of epitopes and alleles

The 3D structure of all T-cell epitopes and crystal structure of their binding alleles were downloaded for peptide-receptor docking. Then molecular docking was conducted using the PatchDock tool, and generated results were refined with the FireDock server. The FireDock server predicted ten structures for individual peptide docking, and we selected the best one following their lower global energy. Among the

Table 2

The selected MHC class-II epitopes for the final vaccine construction.

Epitope	Antigenicity	AS	Allergenicity	Toxicity	Human homology	IFN-gamma	IL-4
AIWFWMWL GARFLEFE	Antigen	1.12	Non-allergen	Non-toxic	Non-homologous	Positive	Inducer
GSRAIWFWMWL GARFL	Antigen	0.74	Non-allergen	Non-toxic	Non-homologous	Positive	Inducer

**Fig. 2.** Figure showing the graphs of the B-cell epitope prediction of the three selected proteins of West Nile Virus. Here, (a) is the graph of epitope prediction for Envelope protein, (b) is the graph of epitope prediction for non-structural protein NS3 and (c) is the graph of epitope prediction for nonstructural protein NS5.**Table 3**

The selected B-cell epitopes for the final vaccine construction.

Epitope	Antigenicity	AS	Allergenicity	Toxicity
KKVIQLNRKSYETEYPKC	Antigen	0.43	Non-allergen	Non-Toxin
GTSDPFPESNAPIS	Antigen	0.40	Non-allergen	Non-Toxin
DTPSPKEYKKGDT	Antigen	0.63	Non-allergen	Non-Toxin
ENEWMEDKTPVERWSDPVYSGKR EDIWCG	Antigen	0.44	Non-allergen	Non-Toxin
IGEEKYVDMSSLRRYEDTIVVED	Antigen	0.47	Non-allergen	Non-Toxin
DKKPRMCSREEFIGKVNSAA	Antigen	0.73	Non-allergen	Non-Toxin
YTKGGPGHEEPQLVQSYG	Antigen	0.55	Non-allergen	Non-Toxin
DLSTRAACPTMGAEAHNEKRADPAFVCKQGVVDRGWGN	Antigen	1.02	Non-allergen	Non-Toxin
QINHHWHKGSSIG	Antigen	0.51	Non-allergen	Non-Toxin

MHC class-I epitopes interaction of FLAVGGVLL with HLA-A*02:01 allele and MSPHRVPNY with HLA-A*01:01 allele showed the best result with the lowest global energy of -64.28 and -62.19 respectively, while GSRAIWFWMWL GARFL of MHC class-II epitopes with HLA-DRB1*01:01 allele provided lowest and best global energy score of -69.14 (Table 4). By analyzing tabulated details, we presented the best three epitopes and their binding interactions with their respective alleles in Fig. 4.

3.6. Construction of multi-epitope subunit vaccine

The vaccine comprised an adjuvant protein, T-cell and B-cell

epitopes, and respective linkers (Table 7). The total number of predicted epitopes utilized in the vaccine were 12 T-cell epitopes and nine linear B-cell epitopes. The TLR4 agonist 50 S ribosomal protein L7/L12 was considered the adjuvant and added to the N-terminal of the vaccine using EAAAK linker to improve immune responses. The epitopes were linked together with AAY, GPGPG, and KK linkers. The final vaccine construct was comprised of 501 amino acid residues (Fig. 5).

3.7. Antigenicity, allergenicity, and physicochemical parameters analysis

The vaccine was found to be probably antigenic with a score of 0.5184, as predicted by the VaxiJen v2.0 server. We also found the

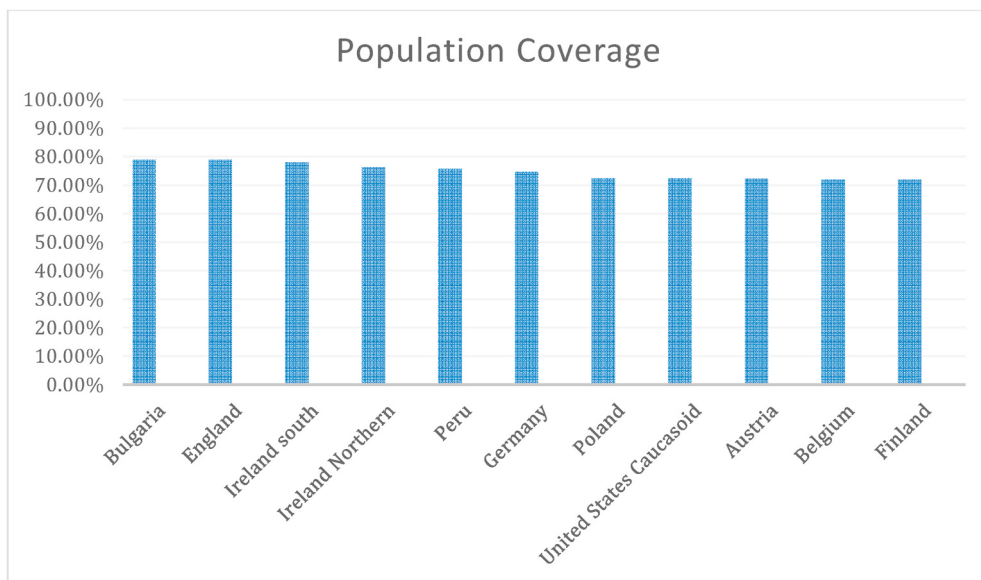


Fig. 3. Population coverage analysis predicted based on the selected T-cell epitopes along with their respective alleles. The selected epitopes showed interactions with a high number of HLA alleles from different countries such as Bulgaria (78.93%), England (78.88%), Ireland South (78.03%), Ireland Northern (76.3%), Peru (75.77%), Germany (74.74%), Poland (72.43%), United States Caucasoid (72.34%), Austria (72.29%), Belgium (71.99%), Finland (71.97%).

Table 4
Docking results between selected epitopes and HLA alleles.

epitopes	HLA allele	Global energy (kcal/mol)
YVGKTVWFV	HLA-A*02:01	-54.52
KGDITTGVY	HLA-A*01:01	-28.85
KTVWFVPSV	HLA-A*02:01	-54.09
MSPHRVPNY	HLA-A*01:01	-62.19
FMWLGARFL	HLA-A*02:01	-31.83
AIWFMWLGARFLEFE	HLA-DRB1*01:01	-45.03
GSRAIWFMWLGARFL	HLA-DRB1*01:01	-69.14
FLAVGGVLL	HLA-A*02:01	-64.28
VLLFLSVNV	HLA-A*02:01	0.03
GMSWITQQL	HLA-A*02:01	-48.41
GTVVLELQY	HLA-A*01:01	-36.80
SVGEKSFVL	HLA-A*02:01	-18.30

vaccine candidate to be non-allergenic as per the prediction of AllerTop. At the same time, other physicochemical properties such as Molecular weight was 54871.91 Da, molecular formula C₂₄₉₁H₃₈₅₉N₆₄₇O₇₁₈S₁₆. Theoretical pI was 8.84, Extinction coefficient was 104,530 M⁻¹cm⁻¹, Instability index was 33.39, Aliphatic index was 73.47, Grand average of hydropathicity (GRAVY) was -0.311 (Table 5).

3.8. Secondary structure prediction

The secondary structural features were evaluated using two different servers. From PRISPRED analysis, we found the vaccine protein comprised of 34.13% alpha-helix, 13.46% beta-strand, and 52.40% random coil regions (Fig. 6). On the other hand, the SIMPA96 server predicted 30.46% alpha-helix, 13.43% beta-strand, and 55.88% random coils of the vaccine construct (Table 6).

3.9. Tertiary structure modeling, refinement, and validation

The 3D structure of the vaccine was modeled through GalaxyWEB. The predicted model was used for further evaluation and refinement. The GalaxyRefine server generated the refined model of the vaccine candidate (Fig. 7). For validation, the Ramachandran plot was used that analyze protein structure. The Ramachandran plot analysis revealed that 95.2% of residues in the protein were found in the favored region.

Additionally, 3.6% of residues in the allowed region and 1.2% of residues in the outlier region (Fig. 8). These Ramachandran plot results indicate the consistency of the vaccine protein structure.

3.10. Vaccine protein disulfide engineering

The disulfide bonds were generated between cysteine residues within the tertiary structure of the vaccine protein. The DbD2 server detected a total of 67 pairs of amino acids capable of forming disulfide bonds. We selected the amino acid pairs having bond energy of less than 2.20 kcal/mol. After evaluation, only six pairs exceeded the criteria shown in Fig. 9 Those amino acid residue pairs were 4 LEU-8 GLU, 16 MET-20 GLU, 112 ALA- 115 GLU, 123 ALA-193 ALA, 147 TYR-201 VAL, and 218 TYR-221 SER. The selected amino acid residues were replaced with a cysteine residue to enable them to form disulfide bonds.

3.11. Protein-protein molecular docking

The molecular docking analysis was executed between vaccine protein and receptor protein (TLR-4). The ClusPro 2.0 and PRODIGY tool of the HADDOCK server was used for the docking study. After performing docking, the ClusPro v2.0 server provided thirty docked complexes, each in a different manner. Then we selected the best-docked complex named cluster 1 with the lowest energy weighted score of -1217.2 in terms of docking interactions pattern between vaccine construct and receptor (Fig. 10a). Furthermore, the docked complex's binding affinity (ΔG) was analyzed by the HADDOCK server with a significant score of -8.3 kcal/mol. The docked complex also was analyzed for binding interactions. The residues participating in binding were Asp490, Thr514, Pro513, Phe487, Glu485, His555, Asn579, Asp580, Ala610, Glu608, Thr611, Ala582, Lys560, Glu586, Met557, Thr558, Ser613, Asp614, Glu586 (Fig. 10b).

3.12. Molecular dynamics study

Normal mode analysis (NMA) was performed to understand the physical movements of atoms and molecules and the stability of the docked complex of the final vaccine construct. The probable deformability generates independent distortion of each residue in the range of 0.1–0.9 Å is depicted by hinges in the chain (Fig. 11a). The B-factor

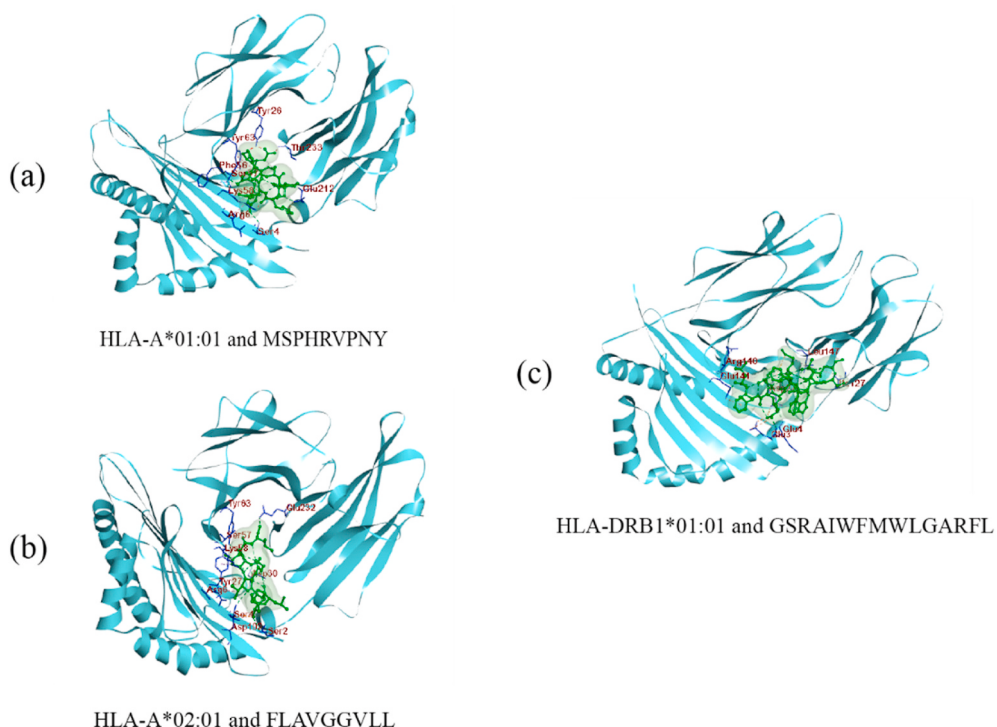


Fig. 4. Figure showing the interactions between the best epitopes from the three proteins and their respective allele. Here, (a) is the interaction between MSPHRVPNY and HLA-A*01:01 allele, (b) is the interaction between FLAVGGVLL and HLA-A*02:01 allele and (c) is the interaction between GSRAIWFWMWL GARFL and HLA-DRB1*01:01 allele.

Table 5
Antigenic, allergenic and physicochemical properties of the vaccine construct.

Characteristics	Finding	Remark
Name of the vaccine	WNV vaccine	–
Total amino acids	501	Suitable
molecular formula	C ₂₄₉₁ H ₃₈₅₉ N ₆₄₇ O ₇₁₈ S ₁₆	–
Antigenicity	(0.5184)	Antigenic
Allergenicity	No	Non-allergen
Molecular weight (Da)	54871.91	Average
Theoretical pI	8.84	Slightly basic
Extinction coefficient (m ⁻¹ cm ⁻¹)	104,530	–
Instability index	33.39	Stable
Aliphatic index	73.47	Thermostable
Grand average of hydropathicity (GRAVY)	-0.311	Hydrophilic

Table 6
The secondary structural features of the vaccine construct.

Features	PSIPRED		SIMPRA96	
	Amino acid	Percentage	Amino acids	Percentage
Alpha helix	142	34.13%	127	30.46%
Beta strand	56	13.46%	56	13.43%
Random coil	218	52.40%	233	55.88%

values deduced by NMA were equivalent to RMS, which explains the comparison between the PDB and the NMA field of the complex (Fig. 11b). The eigenvalue for the complex was found to be 2.899770e-07 (Fig. 11c). In the variance graph, the red-colored bars indicated individual variance, while green-colored bars indicated cumulative variance (Fig. 11d). The co-variance matrix of the complex showed coupling between pairs of residues, where co-related, anti-correlated, or uncorrelated motions represented by red, blue and white colors, respectively (Fig. 11e). It exhibited the interactions of the vaccine and TLR-4 residues and conformational change in the receptor-

binding groove. The molecular dynamics result also provided an elastic network model representing pairs of atoms connected through springs (Fig. 11f). Each dot in the diagram depicted one spring and was colored based on the degree of stiffness, where darker grey regions correspond to the stiffer springs. All these indicative results show complex rigidity, stability, and low deformability of the atoms.

3.13. In silico immune simulation

The immune simulation generated results compatible with actual immune responses. Herein, the secondary and tertiary responses were higher than the primary response. A high concentration of IgM characterized the primary responsibility of the vaccine. The secondary and tertiary responses showed marked increases in the level of IgG1+IgG2, IgM, and IgG + IgM activities with an analogous decrease in antigen level (Fig. 12a). This result revealed the development of the memory cell and consequently increased antigen clearance upon successive exposures (Fig. 12b). Alongside, an elevated response was seen in the cytotoxic T-cell (Fig. 12c) and helper T-cell populations (Fig. 12d) with respective memory development. The increased levels of IFN- γ , IL-12, and IL-10 were also noticed (Fig. 12g). During exposure, enhanced macrophage activity was elucidated (Fig. 12e) with continually proliferating dendritic cells (Fig. 12f).

3.14. Codon optimization and in silico cloning

The regulatory systems responsible for protein expression are different in human and *E. coli* K12 strains. The elementary objective of in silico cloning was to amplify the West Nile Virus-derived vaccine protein into the expression system of *E. coli*. Therefore, the codons of the vaccine construct were adapted by the *E. coli* K12 strain for maximum protein expression. Since the vaccine protein had 501 nucleotides, the reverse transcribed codon sequence was 1503 nucleotides in length. The codon adaptation index (CAI) value, which was 0.979, indicated a surprisingly incredible amount of most abundant codons in the optimized sequence.

Table 7

The sequence composition of the vaccine construct (linkers are in bold letters).

Vaccine construct	No. Of amino acids
MAKLSTDELLDAFKEMTLLELSDFVKKFEETFEVTAAPVAAAAGAAPAGAAVEAAEQQSEFDV ILEAAGDKKIVKVVRIVSGLGLKEAKDLVDGAPKPLLEKVAKEAADAEAKAKLEAAGATVT EAAAKYVGKTVWFVAAYKGDTTGVYAAVYKTVWFVPSVAAYMSPHRVPNYAAFMWL GARFAAYFLAVGGVLLAAYVLLFLSVNVAAYGMSWITQGLAAYGTVVLELQYAAYS GEKSFLV LVGPGPGAIFWMWL GARFL EFGPGP GGSRAIWF MWL GARFL KKKV IQLN RSKY ETEY PKC KK DTPSPKEYKKGD TKKGT SDPF PESNAPI SKKENEW M EDKTPVERWS DPV YSGKREDI WCGKKYTKGGPHEEPQLV QSYGKKIGEEKYD YDYMSSLRYYE DTIVVEDKKDKKPRMC SREEFIG KVNSNAAKKDL STRAAC PTMGEAHNEKRADPAFVCKQGVVDRGWGNKKQINHHWHKGSSIGGGGS	501

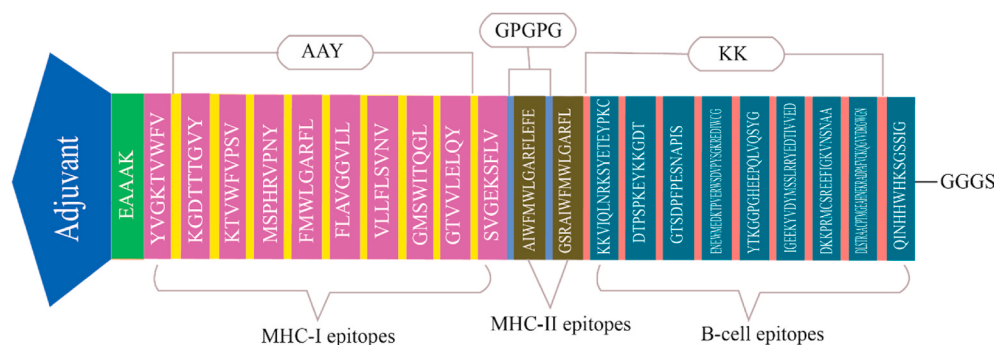


Fig. 5. Graphical map of the formulated multi-epitope vaccine construct. The vaccine constructs included (left to right) an adjuvant, MHC class-I, MHC class-II and B-cell epitopes are shown in the dark blue, violet, olive green and blue-green rectangular boxes. Herein, the adjuvant and the MHC class-I epitope were linked by EAAAK linker (green), MHC class-I epitopes were added together by AYY linkers (yellow), MHC class-II epitopes by GPGPG linkers (sky-blue), and B-cell epitopes by KK linkers (brown-red).

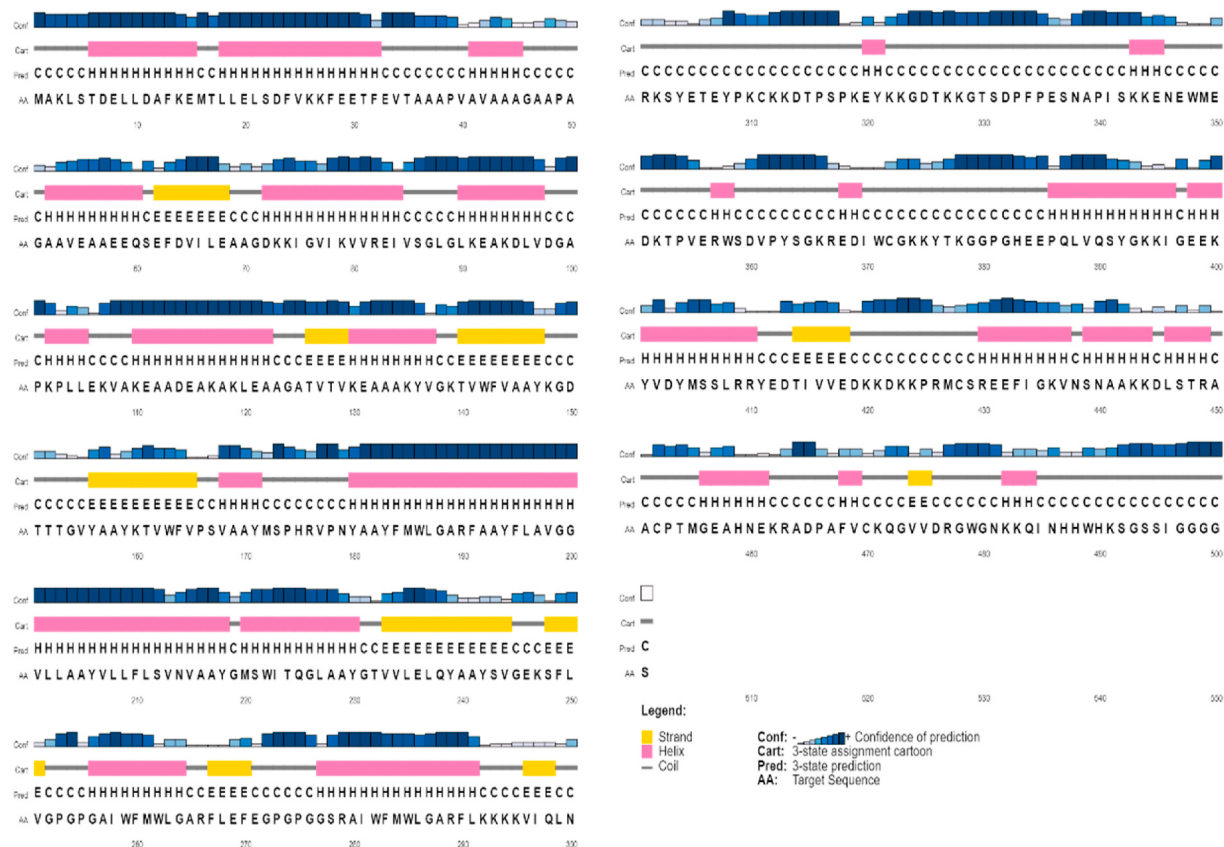


Fig. 6. Secondary structure prediction of constructed WNV vaccine protein using PSIPRED server.

A significant GC content of the optimized sequence was also found to be 48.23% which remained within the optimum range. Before inserting the sequence into the pET28a (+) vector, EcoR1, and Xho1 restriction sites

were added at the N-terminal and C-terminal, respectively, in the adapted sequence. Finally, the codon sequences were inserted and cloned into the pET28a (+) cloning vector. Thus, the final length of the

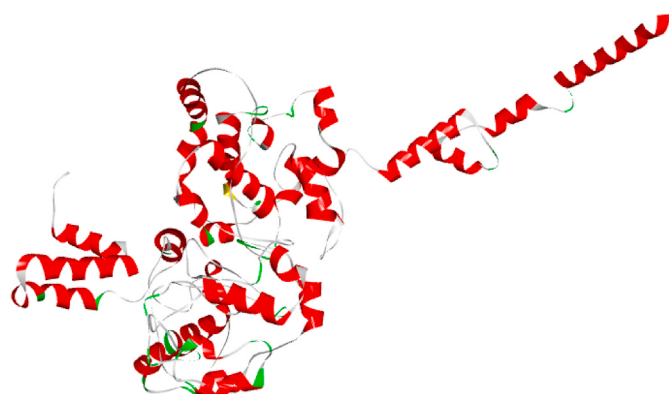


Fig. 7. The tertiary structure of the WNV vaccine predicted by GalaxyWEB server and refined by GalaxyRefine server.

cloning vector was 6.842 kbp (Fig. 13).

4. Discussion

Vaccine proves to be a secure and effective measure to confine the prevalence of deadly contagious diseases and to save millions of lives. Through the advancement of sequencing technology and several bioinformatics tools, we have adequate data and information about the genomics of different infectious pathogens. The availability of genome sequences has resulted in the rapid identification of genes and proteins that could be possible targets for the design of drugs or vaccines. Bioinformatics has played a crucial role in predicting potential vaccine candidates, accelerating vaccine development alongside saving costs [43]. These automated tools can analyze the whole proteome to find immunogenic proteins, B and T cell epitope, immunity inducing properties, and so on [106,107]. This immunoinformatics technique has been exploited to design an epitope-based vaccine for various viral, bacterial,

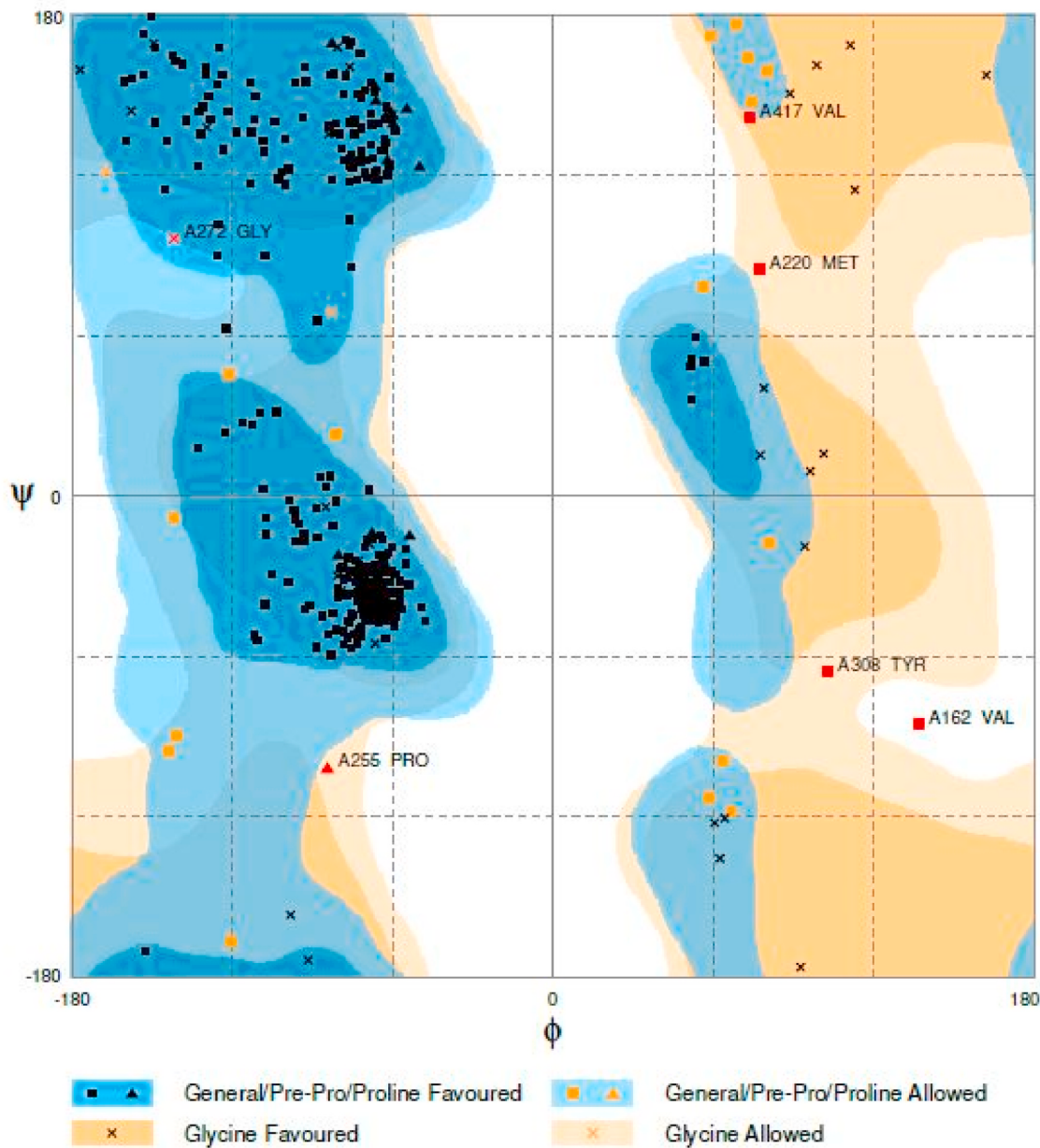


Fig. 8. The Ramachandran plot analysis of the WNV vaccine construct. The Ramachandran plot statistics represent the most favorable, accepted, and disallowed regions with a percentage of 95.2%, 3.6%, and 1.2%, respectively.

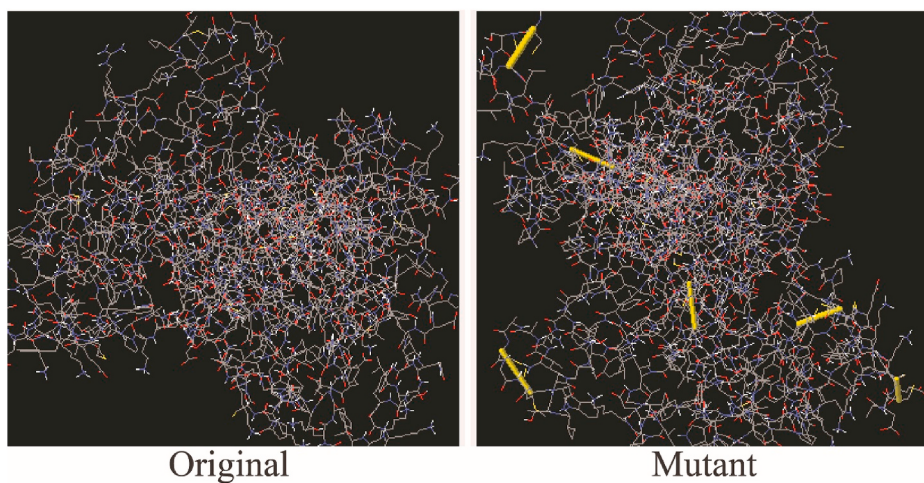


Fig. 9. The disulfide engineering of the WNV vaccine construct, both the original (left) and mutant (right) forms are shown.

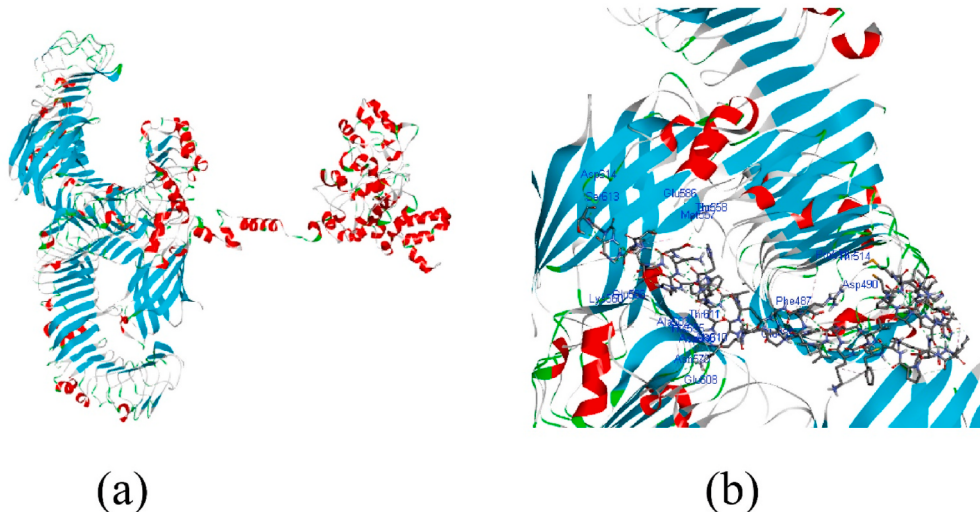


Fig. 10. (A) Molecular docking between the WNV vaccine and the TLR4 receptor. (b) The residues participating in binding were Asp490, Thr514, Pro513, Phe487, Glu485, His555, Asn579, Asp580, Ala610, Glu608, Thr611, Ala582, Lys560, Glu586, Met557, Thr558, Ser613, Asp614, Glu586.

fungal, and parasitic infections [35,48,108–110]. Hence, it is possible to design multi-epitope vaccines based on immunogenic epitopes by simply utilizing various bioinformatics methods and tools. Though the prediction accuracy of potential vaccine and their translation into *in vivo/in vitro* conditions still requires improvement, it significantly enhances the efficacy in the effort, time, and money.

The use of bioinformatics tools has significantly accelerated the development of new vaccine targets. In this study, we designed a peptide-based subunit vaccine that can combat against West Nile Virus by utilizing the reverse vaccinology approach. As E, C, and NS proteins play a vital role in immune invasion and viral replication, our motive was to design a multi-epitope vaccine by targeting these proteins. We retrieved viral proteins of WNV by means of the National Center for Biotechnology Information (NCBI) database. The appropriate antigenic protein sequences were selected for further analysis by analyzing their antigenicity, allergenicity, and other physicochemical features. After selecting protein sequences, the T-cell (MHC-1 & MHC-2) and B-cell epitopes were predicted and evaluated for vaccine construction. The competent epitopes of the selected proteins were predicted based on antigenic, non-allergenic, and non-toxic features. The cytokines, interferon (IFN- γ , IL-4) induction capacity were also determined for MHC-2 epitopes. T-cell epitope enables recognizing antigens where the B-cell

epitope is the part of the antigen engaged in binding to the immunoglobulin or antibody [111,112]. Population coverage analysis of T-cell epitopes and their respective HLA binding alleles were also enumerated using the IEDB server. HLA alleles are highly polymorphic, and worldwide distributions of HLA alleles serve the vaccine efficiently across the globe [75,113]. The maximum result of population coverage was recorded at 78.93% in Bulgaria. A docking study was performed to assure the binding capability of the epitopes with their respective HLA molecules. For the docking purpose, a 3D model of epitopes and crystal structure of HLA alleles were downloaded and then submitted into the FireDock server to generate binding interactions. Epitopes FLAVGGVLL with HLA-A*02:01 allele and MSPHRVPNY with HLA-A*01:01 allele were generating the best result with the lowest global energy of -64.28 and -62.19, respectively, where GSRAIWFMLGARFL of MHC class-II epitopes generated the lowest global energy score of -69.14.

The selected T-cell and B-cell epitopes were subjected to design a vaccine molecule. The vaccine protein was constructed using incondite epitopes, suitable adjuvant, and respective linkers. An adjuvant is a substance that can enhance the effectiveness of vaccines by provoking strong immune responses [114]. The TLR4 agonist 50 S ribosomal protein L7/L12 was selected as an adjuvant, and AAY, GPGPG, and KK linkers combined the vaccine sequence to develop a multi-epitope

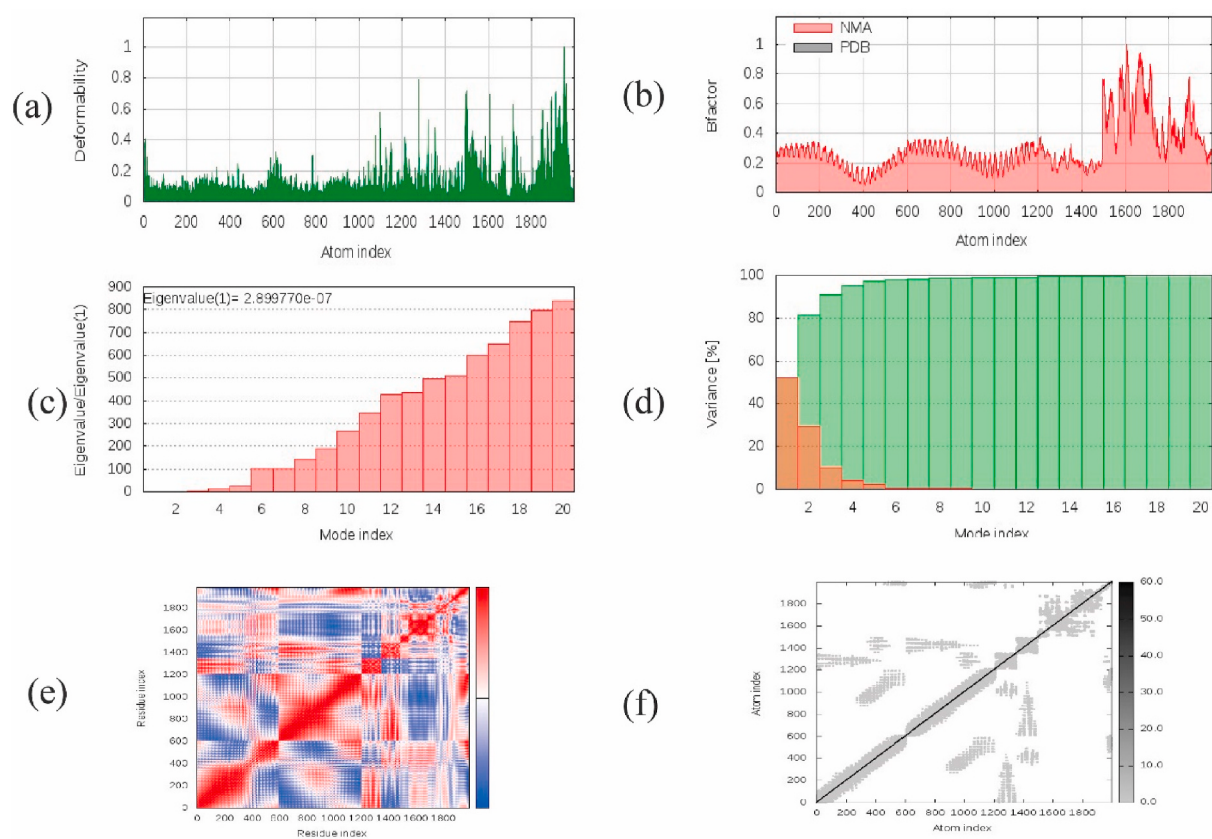


Fig. 11. The results of molecular dynamics simulation study of WNV vaccine and TLR-4 docked complex. Here, (a) deformability, (b) B-factor, (c) eigenvalues, (d) variance (red color indicates individual variances and green color indicates cumulative variances), (e) co-variance map (correlated (red), uncorrelated (white) or anti-correlated (blue) motions) and, (f) elastic network (darker grey regions indicate more stiffer regions).

vaccine protein. The vaccine construct was found to be antigenic, non-allergenic and the protein's physicochemical features predicted it to be hydrophilic, stable, and basic in nature. The secondary structural features revealed that the vaccine molecule had amino acids with more than 30% alpha-helix formation, more than 13% beta-sheet, and coil structures over 50%. The refinement and validation studies demonstrated that the vaccine is stable, where 95.2% of amino acid residues were found in the most favored regions. The six pairs of amino acid residues were found to be generated disulfide bonds in between cysteine residue. The disulfide bonds are significant for protein folding and stability [115,116].

The molecular docking was carried out with the objective to assay the immune response of TLR-4 against our predicted vaccine protein. Molecular docking study of protein-receptor complex generated the lowest energy weighted score of -1217.2 and binding affinity (ΔG) with a score of -8.3 kcal/mol. These docking results ensured the chance of infection inhibitory alacrity of the predicted vaccine and indicated a probable compact interaction within the protein-receptor complex. Further, the physical movement and stabilization of the docked complex were assessed by molecular dynamics study. According to the eigenvalue and deformability results, the complex should be stable in the biological environment. Besides, the immune simulation was also conducted to observe the vaccine's immune response to combat the virus. The immune simulation study shared compatible results with ordinary immune reactions. The high levels of immunoglobulin activities were seen in the secondary and tertiary responses. The development of T-cell and B-cell populations was significant.

Furthermore, both macrophage and dendritic cell activity were favorable in our study. Finally, codon optimization and in-silico cloning of the vaccine protein sequence were carried out, respectively. In order to achieve a high level of expression, the codon was optimized according

to the *E. coli* K12 strain. Both the codon adaptation index (CAI) and GC content were significant for maximum protein expression in *E. coli*. The adapted codons were then incorporated into the pET28a (+) vector which, could efficiently encode vaccine protein in the *E. coli* host. We recommend further wet-lab associated research using model organisms for empirical validation of our predicted vaccine.

5. Conclusion

This study aimed to design a safe, potent, and effective immunogenic multi-epitope vaccine that may have the caliber to prevent West Nile Virus. Our predicted vaccine protein can stimulate humoral, innate, and cellular immunity. However, this study suggests further empirical validation to vindicate this work. The identified potential T-cell and B-cell epitopes can be used for subsequent investigations. We believe that our proposed vaccine candidate will exhibit considerable results against WNV in practice.

Author's contribution

MWA: Conceptualization, Project administration, Experiment Design, Manuscript writing, and Draft Preparation. MNS: Data Handling, Data Analysis and writing. KMS: Data Handling, Data analysis and Graphical design. FA: Data Handling and Data Analysis. Md. Wasim Alom (MWA), Mobasshir Noor Shehab (MNS), Khaled Mahmud Sujon (KMS), Farzana Akter (FA).

Funding statement

This research did not receive any specific grant from funding agencies in the public, commercial, or non-profit sectors.

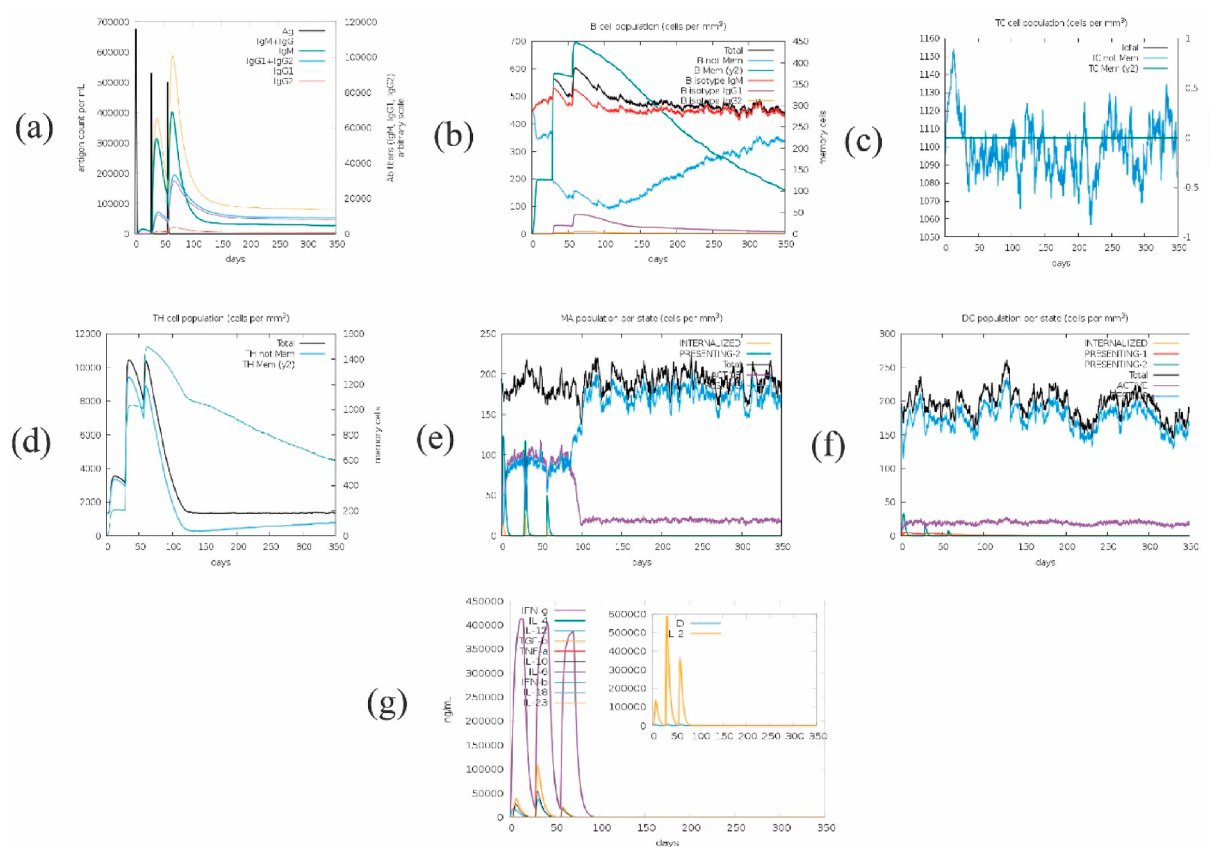


Fig. 12. Immune response triggered by the predicted vaccine as antigen, showing (a) Immunoglobulin production in response to antigen injection, (b) B-cell population, (c) cytotoxic T-cell population, (d) helper T-cell population, (e) macrophages population per state, (f) dendritic cell population per state, (g) induction of cytokines and interleukins with Simpson index.

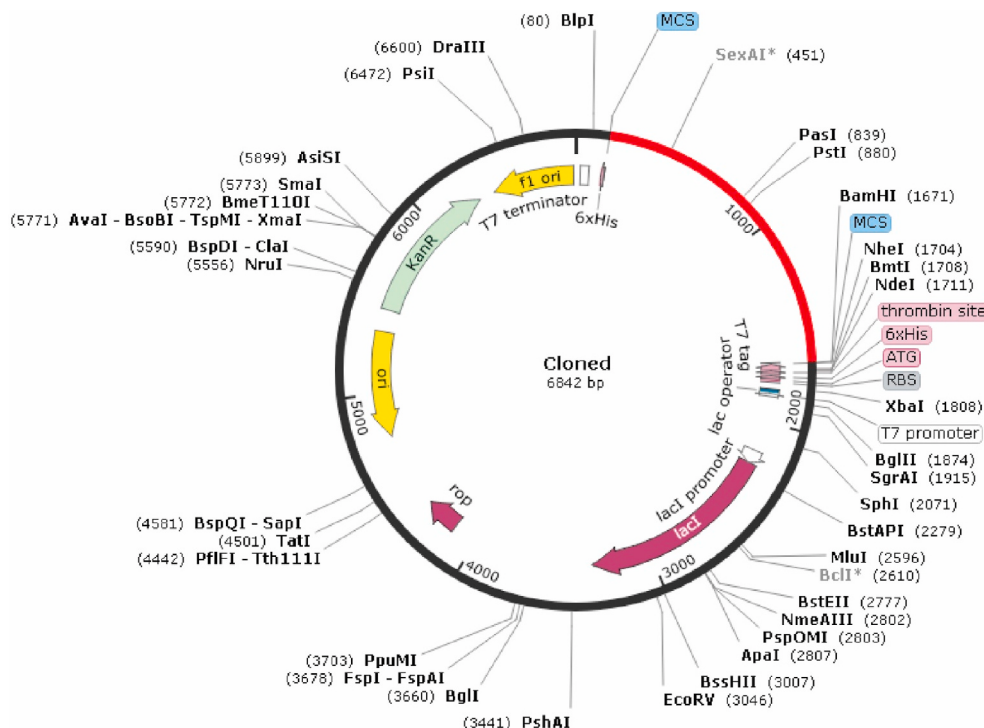


Fig. 13. The in silico cloning of the designed vaccine into the pET-28a (+) vector. Herein, black color represents the vector DNA, while the red color indicates the adapted DNA sequence of the designed vaccine.

Declaration of competing interest

The authors declare that they have no known competing financial interests or personal relationships that could have appeared to influence the work reported in this paper.

Acknowledgement

We express our gratitude and thanks to Allah, our parents, teachers and friends.

References

- [1] Proc MC, Virus WN, Clinic M, Clinic M. September. West Nile virus: epidemiology, clinical presentation, diagnosis, and prevention, 78; 2003. p. 1137–44.
- [2] Smithburn KC, Hughes TP, Burke AW, Paul JH. A neurotropic virus isolated from the blood of a native of Uganda 1. Am J Trop Med Hyg 1940;s1–20(4):471–92. <https://doi.org/10.4269/ajtmh.1940.s1-20.471>.
- [3] Bernkopf H, Levine S, Nerson R. Isolation of West nile virus in Israel. J Infect Dis Jul. 1953;93(3):207–18. <https://doi.org/10.1093/infdis/93.3.207>.
- [4] Lanciotti RS, et al. Origin of the West Nile virus responsible for an outbreak of encephalitis in the Northeastern United States. Science 84 1999;286(5448): 2333–7. <https://doi.org/10.1126/science.286.5448.2333>.
- [5] Gancz AY, Barker IK, Lindsay R, Dibbernardo A, McKeever K, Hunter B. “West Nile virus outbreak in north American owls, ontario, 2002,” *emerg. Inf Dis* 2004;10 (12):2135–42. <https://doi.org/10.3201/eid1012.040167>.
- [6] Hernández-triana LM, Jeffries CL, Mansfield KL, Carnell G, Fooks AR, Johnson N. Emergence of West Nile virus lineage 2 in Europe : a review on the introduction and spread of a mosquito-borne disease. December 2014;2:1–8. <https://doi.org/10.3389/fpubh.2014.00271>.
- [7] Mitchell J, Fellow AC. West Nile encephalitis by professor tom solomon. Chair of Neurological Science , University of Liverpool and Katherine Dodd , Specialist Registrar in Neurology and reviewed, 2016;1–3.
- [8] Troupin A, Colpitts TM. Overview of West nile virus transmission and epidemiology. Methods Mol Biol 2016;1435:15–8. https://doi.org/10.1007/978-1-4939-3670-0_2.
- [9] Gould LH, Fikrig E. West Nile virus: a growing concern? J Clin Invest 2004;113 (8):1102–7. <https://doi.org/10.1172/JCI21623>.
- [10] Hayes EB, Komar N, Nasci RS, Montgomery SP, Leary DRO, Campbell GL, Hayes. Epidemiology and transmission dynamic of West nile virus disease 2005;11(8). 2005.
- [11] Gyure KA. West nile virus infections. J Neuropathol Exp Neurol 2009;68(10): 1053–60. <https://doi.org/10.1097/NEN.0b013e3181b88114>.
- [12] Brinton MA. T he M OLECULAR B iology OF W est N ile V IRUS : a new invader of the western hemisphere. 2002. p. 371–402. <https://doi.org/10.1146/annurev.micro.56.012302.160654>.
- [13] Mukhopadhyay S, Kim B, Chipman PR, Rossmann MG, Kuhn RJ. October. Structure of West nile virus, 302; 2003. 2003.
- [14] Saiz J. World J Virol 2012;1(2):51–70. <https://doi.org/10.5501/wjv.v1.i2.51>.
- [15] B. Londono-renteria and T. M. Colpitts, “Chapter 1 A brief review of West nile virus biology,” vol. 1435, doi: 10.1007/978-1-4939-3670-0.
- [16] De Filette M, Ulbert S, Diamond MS, Sanders NN. Recent progress in West Nile virus diagnosis and vaccination. 2012. p. 1–15.
- [17] Hussmann KL, Vandergaast R, Zheng K, Hoover LI, Fredericksen BL. Structural proteins of West Nile virus are a major determinant of infectious particle production and fitness in astrocytes. PART 9 J Gen Virol 2014;95:1991–2003. <https://doi.org/10.1099/vir.0.065474-0>.
- [18] Cola G. Gene mapping and positive identification of the non-structural proteins NS2A , NS2B , NS3 , NS4B and NS5 of the flavivirus kunjin and their cleavage sites. 1988. p. 23–34.
- [19] Wengler G, Castle E, Leidner U, Nowak T, Wengler G. Sequence analysis of the membrane protein V3 of the flavivirus West Nile virus and of its gene 1985;274: 264–74.
- [20] Wengler G, Wengler G. Primary structure of the West nile flavivirus genome region coding for all nonstructural proteins, 26; 1986. p. 10–26.
- [21] Londono-renteria B, Colpitts TM. June. Chapter 1 A brief review of West nile virus biology, 1435. “ Springer Link; 2016. p. 1–13. <https://doi.org/10.1007/978-1-4939-3670-0>.
- [22] Colpitts TM, Conway MJ, Montgomery RR, Fikrig E. West Nile virus: biology, transmission, and human infection. Clin Microbiol Rev 2012;25(4):635–48. <https://doi.org/10.1128/CMR.00045-12>.
- [23] Khromykh AA, Westaway EG. RNA binding properties of core protein of the flavivirus Kunjin. Arch Virol 1996;141(3–4):685–99. <https://doi.org/10.1007/BF01718326>.
- [24] Stiasny K, Heinz FX. Flavivirus membrane fusion. J Gen Virol 2006;87(10): 2755–66. <https://doi.org/10.1099/vir.0.82210-0>.
- [25] Smit JM, Moesker B, Rodenhuis-Zybert I, Wilschut J. Flavivirus cell entry and membrane fusion. Viruses 2011;3(2):160–71. <https://doi.org/10.3390/v3020160>.
- [26] Shiryaev SA, Chernov AV, Aleshin AE, Shiryaeva TN, Strongin AY. NS4A regulates the ATPase activity of the NS3 helicase: a novel co-factor role of the non-structural protein NS4A from West Nile virus. J Gen Virol 2009;90(9): 2081–5. <https://doi.org/10.1099/vir.0.012864-0>.
- [27] Borowski P, et al. Purification and characterization of West nile virus nucleoside triphosphatase (NTPase)/Helicase: evidence for dissociation of the NTPase and helicase activities of the enzyme. J Virol 2001;75(7):3220–9. <https://doi.org/10.1128/jvi.75.7.3220-3229.2001>.
- [28] Flamand M, Megret F, Mathieu M, Lepault J, Rey FA, Deubel V. Dengue virus type 1 nonstructural glycoprotein NS1 is secreted from mammalian cells as a soluble hexamer in a glycosylation-dependent fashion. J Virol 1999;73(7):6104–10. <https://doi.org/10.1128/jvi.73.7.6104-6110.1999>.
- [29] Popescu CP, et al. “Re-emergence of severe West Nile virus neuroinvasive disease in humans in Romania, 2012 to 2017—implications for travel medicine,” *Travel Med. Inf Disp* 2018;22:30–5. <https://doi.org/10.1016/j.tmaid.2018.03.001>.
- [30] Hayes EB, Sejvar JJ, Zaki SR, Lanciotti RS, Bode AV, Campbell GL. Virology, pathology, and clinical manifestations of West Nile virus disease. *Emerg Infect Dis* 2005;11(8):1174–9. <https://doi.org/10.3201/eid1108.050289b>.
- [31] Centers for Disease Control and Prevention (Cdc). “Morbidity and mortality weekly report surveillance for human West Nile virus disease — United States , 1999 – 2008 . MMWR Wkly. Rep. 2008;59(31):1999. 2010.
- [32] Lindsey NP, Staples JE, Lehman JA, Fischer M. Medical risk factors for severe West Nile virus disease, United States, 2008–2010. Am J Trop Med Hyg 2012;87 (1):179–84. <https://doi.org/10.4269/ajtmh.2012.12-0113>.
- [33] ” [Online]. Available: <https://www.cdc.gov/westnile/>.
- [34] Zhang L. “Multi-epitope vaccines: a promising strategy against tumors and viral infections.” *Cell. Mol Immunol* 2018;15(2):182–4. <https://doi.org/10.1038/cmi.2017.92>.
- [35] Shey RA, et al. In-silico design of a multi-epitope vaccine candidate against onchocerciasis and related filarial diseases. *Sci Rep* 2019;9(1):1–18. <https://doi.org/10.1038/s41598-019-40833-x>.
- [36] Alam Khan M, Kang Y-M. WITHDRAWN: enhancement of open circuit voltage in organic solar cell by employing an ambipolar polymer as a controlled additive. *J. Saudi Chem. Soc.* 2014;9:361–71. <https://doi.org/10.1016/j.jscs.2014.12.002>.
- [37] Buonaguro L. Developments in cancer vaccines for hepatocellular carcinoma. *Cancer Immunol Immunother* 2016;65(1):93–9. <https://doi.org/10.1007/s00262-015-1728-y>.
- [38] Lu C, et al. A novel multi-epitope vaccine from MMA-1 and DKK1 for multiple myeloma immunotherapy. *Br J Haematol* 2017;178(3):413–26. <https://doi.org/10.1111/bjh.14686>.
- [39] Kumar N, Sood D, van der Spek PJ, Sharma HS, Chandra R. Molecular binding mechanism and pharmacology comparative analysis of noscapine for repurposing against SARS-CoV-2 protease. *J Proteome Res* 2020;19(11):4678–89. <https://doi.org/10.1021/acs.jproteome.0c00367>.
- [40] Kumar N, Sood D, Sharma N, Chandra R. Multiepitope subunit vaccine to evoke immune response against acute encephalitis. *J Chem Inf Model* 2020;60(1): 421–33. <https://doi.org/10.1021/acs.jcim.9b01051>.
- [41] Nosrati M, Mohabatkar H, Behbahani M. A novel multi-epitope vaccine for cross protection against hepatitis C virus (HCV): an immunoinformatics approach. *Res. Mol. Med.* 2017;5(1):17–26. <https://doi.org/10.29252/rmm.5.1.17>.
- [42] Islam R, Parvez MSA, Anwar S, Hosen MJ. Delineating blueprint of an epitope-based peptide vaccine against the multiple serovars of dengue virus: a hierarchical reverse vaccinology approach. *May Informatics Med. Unlocked* 2020; 20. <https://doi.org/10.1016/j.jimu.2020.100430>.
- [43] Dash R, Das R, Junaid M, Akash MFC, Islam A, Hosen SMZ. In silico-based vaccine design against Ebola virus glycoprotein. *Adv. Appl. Bioinforma. Chem.* 2017;10 (1):11–28. <https://doi.org/10.2147/AABC.S115859>.
- [44] Na S, P B, K K. Immunoinformatics aided prediction of cytotoxic T cell epitope of respiratory. *Synthetic Virus* 2015;1(2):99–104.
- [45] Bin Sayed S, Nain Z, Khan MSA, Abdulla F, Tasmin R, Adhikari UK. Exploring Lassa virus proteome to design a multi-epitope vaccine through immunoinformatics and immune simulation analyses. *Int J Pept Res Therapeut* 2020;26(4):2089–107. <https://doi.org/10.1007/s10989-019-10003-8>.
- [46] Usman Mirza M, et al. Towards peptide vaccines against Zika virus: immunoinformatics combined with molecular dynamics simulations to predict antigenic epitopes of Zika viral proteins. *December Sci Rep* 2016;6:1–18. <https://doi.org/10.1038/srep37313>.
- [47] Srivastava S, et al. Design of novel multi-epitope vaccines against severe acute respiratory syndrome validated through multistage molecular interaction and dynamics. *J Biomol Struct Dyn* 2019;37(16):4345–60. <https://doi.org/10.1080/07339110.2018.1548977>.
- [48] Ikram A, et al. Exploring NS3/4A , NS5A and NS5B proteins to design conserved subunit multi-epitope vaccine against HCV utilizing immunoinformatics approaches. *Sci Rep* 2018;(October):1–14. <https://doi.org/10.1038/s41598-018-34254-5>.
- [49] Schleinkofer K, Wang T, Wade RC. Molecular docking. *Encycl. Ref. Genomics Proteomics Mol. Med.* 2006;443:1149–53. https://doi.org/10.1007/3-540-29623-9_3820.
- [50] Singh A, Kumar N, Sood D, Singh S, Awasthi A, T V, Chandra* R. Designing of a novel indoline scaffold based antibacterial compound and pharmacological evaluation using chemoinformatics approach. *Curr Top Med Chem* 2018;18(23): 2056–65. <https://doi.org/10.2174/156802661966181129125524>.
- [51] Kumar N, Sood D, Tomar R, Chandra R. Antimicrobial peptide designing and optimization employing large-scale flexibility analysis of protein-peptide fragments. *ACS Omega* 2019;4(25):21370–80. <https://doi.org/10.1021/acsomega.9b03035>.

- [52] Geng H, Chen F, Ye J, Jiang F. Applications of molecular dynamics simulation in structure prediction of peptides and proteins. *Comput Struct Biotechnol J* 2019; 17:1162–70. <https://doi.org/10.1016/j.csbj.2019.07.010>.
- [53] Kumar N, et al. Antitussive noscapine and antiviral drug conjugates as arsenal against COVID-19: a comprehensive chemoinformatics analysis. *J Biomol Struct Dyn* 2020;1–16. <https://doi.org/10.1080/07391102.2020.1808072>.
- [54] Kumar N, Sood D, Singh S, Kumar S, Chandra R. High bio-recognizing aptamer designing and optimization against human herpes virus-5. *Eur J Pharmaceut Sci* July 2020;156:105572. <https://doi.org/10.1016/j.ejps.2020.105572>. 2021.
- [55] Petersen LR. “West Nile Virus: a reemerging global pathogen” 2001;7(4):611–4.
- [56] Kaufusi PH, Tseng A, Nerurkar VR, Microbiology M, Burns JA. *HHS Public Access* 2017;:45–60. <https://doi.org/10.1007/978-1-4939-3670-0>. 2017.
- [57] Wilson JR, de Sessions PF, Leon MA, Scholla F. West Nile virus nonstructural protein 1 inhibits TLR3 signal transduction. *J Virol* 2008;82(17):8262–71. <https://doi.org/10.1128/jvi.00226-08>.
- [58] Malet H, et al. Crystal structure of the RNA polymerase domain of the West Nile virus non-structural protein 5. *J Biol Chem* 2007;282(14):10678–89. <https://doi.org/10.1074/jbc.M607273200>.
- [59] Chappell K, Stoermer M, Fairlie D, Young P. West Nile virus NS2B/NS3 protease as an antiviral target. *Curr Med Chem* 2008;15(27):2771–84. <https://doi.org/10.2174/092986708786242804>.
- [60] Doytchinova IA, Flower DR. Identifying candidate subunit vaccines using an alignment-independent method based on principal amino acid properties. *Vaccine* 2007;25(5):856–66. <https://doi.org/10.1016/j.vaccine.2006.09.032>.
- [61] Doytchinova IA, Flower DR. Bioinformatic approach for identifying parasite and fungal candidate subunit vaccines. *Open Vaccine* 2010;3(1):22–6. <https://doi.org/10.2174/1875035400801010022>.
- [62] Doytchinova IA, Flower DR, VaxiJen “. A server for prediction of protective antigens, tumour antigens and subunit vaccines. *BMC Bioinf* 2007;8(-7):1. <https://doi.org/10.1186/1471-2105-8-4>.
- [63] Wilkins MR, et al. Protein identification and analysis tools in the ExPASy server. *Methods Mol Biol* 1999;112:531–52. https://doi.org/10.1385/1-59259-584-7_531.
- [64] Kumar BV, Connors TJ, Farber DL. Human T cell development, localization, and function throughout life. *Immunity* 2018;48(2):202–13. <https://doi.org/10.1016/j.jimmuni.2018.01.007>.
- [65] Sigal LJ, Crotty S, Andino R, Rock KL. Cytotoxic T-cell immunity to virus-infected non-haematopoietic cells requires presentation of exogenous antigen. *Nature* 1999;398(6722):77–80. <https://doi.org/10.1038/18038>.
- [66] Behrens G, et al. Helper T cells, dendritic cells and CTL Immunity. *Immunol Cell Biol* 2004;82(1):84–90. <https://doi.org/10.1111/j.1440-1711.2004.01211.x>.
- [67] Kuroaki T, Kometani K, Ise W. Memory B cells. *Nat Rev Immunol* 2015;15(3): 149–59. <https://doi.org/10.1038/nri3802>.
- [68] Jurtz V, Paul S, Andreatta M, Marcattili P, Peters B, Nielsen M. “NetMHCpan-4.0: improved peptide–MHC class I interaction predictions integrating eluted ligand and peptide binding affinity data. *J Immunol* 2017;199(9):3360–8. <https://doi.org/10.4049/jimmunol.1700893>.
- [69] Moutafchi M, et al. A consensus epitope prediction approach identifies the breadth of murine CD8+ cell responses to vaccinia virus. *Nat Biotechnol* 2006;24(7): 817–9. <https://doi.org/10.1038/nbt1215>.
- [70] Jespersen MC, Peters B, Nielsen M, Marcattili P. BepiPred-2.0: improving sequence-based B-cell epitope prediction using conformational epitopes. *Nucleic Acids Res* 2017;45(W1):W24–9. <https://doi.org/10.1093/nar/gkx346>.
- [71] Dimitrov I, Bangov I, Flower DR, Doytchinova I, “AllerTOP v. 2 - a server for in silico prediction of allergens. *J Mol Model* 2014;20(6). <https://doi.org/10.1007/s00894-014-2278-5>.
- [72] Gupta S, Kapoor P, Chaudhary K, Gautam A, Kumar R, Raghava GPS. In silico approach for predicting toxicity of peptides and proteins. *PLoS One* 2013;8(9). <https://doi.org/10.1371/journal.pone.0073957>.
- [73] Dhanda SK, Vir P, Raghava GPS. Designing of interferon-gamma inducing MHC class-II binders. *Biol Direct* 2013;8(1):1–15. <https://doi.org/10.1186/1745-6150-8-30>.
- [74] Dhanda SK, Gupta S, Vir P, Raghava GP. Prediction of IL4 inducing peptides. *Clin Dev Immunol* 2013;263952. <https://doi.org/10.1155/2013/263952>. 2013.
- [75] Bui HH, Sidney J, Dinh K, Southwood S, Newman MJ, Sette A. Predicting population coverage of T-cell epitope-based diagnostics and vaccines. *BMC Bioinf* 2006;7(–5):1. <https://doi.org/10.1186/1471-2105-7-153>.
- [76] Lamiable A, Thévenet P, Rey J, Vavrusa M, Derreumaux P, Tufféry P, Pep-Fold3 “. Faster de novo structure prediction for linear peptides in solution and in complex. *Nucleic Acids Res* 2016;44(W1):W449–54. <https://doi.org/10.1093/nar/gkw329>.
- [77] Berman HM, et al. The protein data bank. *Acta Crystallogr Sect D Biol Crystallogr* 2002;58(6):899–907. <https://doi.org/10.1107/S0907444902003451>.
- [78] L DeLand W, Pymol “. An open-source molecular graphics tool,” {CCP4} Newslett. Protein Crystallogr 2002;40:1–8 [Online]. Available: http://www ccp4.ac.uk/newsletters/newsletter40/11_pymol.pdf.
- [79] Duhovny D, Nussinov R, Wolfson HJ. Efficient unbound docking of rigid molecules. *Lect Notes Comput Sci (including Subser Lect Notes Artif Intell Lect Notes Bioinformatics)* 2002;2452:185–200. https://doi.org/10.1007/3-540-45784-4_14.
- [80] Andrusier N, Nussinov R, Wolfson HJ. Molecular docking”. August 2006. p. 139–59. <https://doi.org/10.1002/prot>. 2007.
- [81] Studio D. Dassault systemes BIOVIA, Discovery Studio modelling environment, release4.5. Accelrys Softw. Inc.; 2015.
- [82] Borthwick N, Silva-arrieta S, Llano A, Takiguchi M, Brander C. “Novel nested peptide epitopes recognized by CD4 + T cells induced by HIV-1 conserved-region vaccines.”. 2020.
- [83] Farhadi T, Nezafat N, Ghasemi Y, Karimi Z. Designing of complex multi-epitope peptide vaccine based on omgs of Klebsiella pneumoniae: an in silico approach. *Int J Pept Res Therapeut* 2015;325–41. <https://doi.org/10.1007/s10989-015-9461-0>.
- [84] Abdellrazeq GS, et al. Simultaneous cognate epitope recognition by bovine CD4 and CD8 T cells is essential for primary expansion of antigen-specific cytotoxic T-cells following ex vivo stimulation with a candidate *Mycobacterium avium* subsp. *paratuberculosis* peptide vaccine. *Vaccine* 2019;(xxxx):4–13. <https://doi.org/10.1016/j.vaccine.2019.12.052>.
- [85] Taylor P, Street M, Wt L. In silico design of a DNA-based HIV-1 multi-epitope vaccine for Chinese populations., 2015. p. 37–41. <https://doi.org/10.1080/21645515.2015.1012017>.
- [86] Nezafat N, Karimi Z, Eslami M, Mohkam M. Designing an efficient multi-epitope peptide vaccine against *Vibrio cholerae* via combined immunoinformatics and protein interaction based approaches. *Comput Biol Chem* 2016;62:82–95. <https://doi.org/10.1016/j.combiolchem.2016.04.006>.
- [87] Jones DT. Protein secondary structure prediction based on position-specific scoring matrices. *J Mol Biol* 1999;292(2):195–202. <https://doi.org/10.1006/jmbi.1999.3091>.
- [88] Levin JM, Robson B, Garnier J. An algorithm for secondary structure determination in proteins based on sequence similarity. *FEBS Lett* 1986;205(2): 303–8. [https://doi.org/10.1016/0014-5793\(86\)80917-6](https://doi.org/10.1016/0014-5793(86)80917-6).
- [89] Ko J, Park H, Heo L, Seok C. GalaxyWEB server for protein structure prediction and refinement. *Nucleic Acids Res* 2012;40(W1):294–7. <https://doi.org/10.1093/nar/gks493>.
- [90] Nugent T, Cozzetto D, Jones DT. Evaluation of predictions in the CASP10 model refinement category. *Proteins Struct Funct Bioinforma*. 2014;82(SUPPL.2): 98–111. <https://doi.org/10.1002/prot.24377>.
- [91] Lovell SC, , et al. IAltschul S, Gish W, Miller W, Myers W, D J Lipman. (1990). Basic local alignment search tool. *Journal of molecular Biology.etry: phi,psi and C beta deviation. Structure validation by C alpha geomFE., editor. Proteins-Structure Funct. Genet.* August 2002;50:437–50. <https://doi.org/10.1002/prot.10286>. 2003.
- [92] Craig DB, Dombrowski AA. Disulfide by Design 2.0: a web-based tool for disulfide engineering in proteins. *BMC Bioinf* 2013;14(1):1–6. <https://doi.org/10.1186/1471-2105-14-346>.
- [93] Park Kinam. 基因的改变NIH public access. *Bone* 2014;23(1):1–7. <https://doi.org/10.1038/jid.2014.371>.
- [94] Benjamin MJS, Davis M, Rall Glen F. “乳鼠心肌提取 HHS public access. *Physiol Behav* 2017;176(1):139–48. <https://doi.org/10.1016/j.physbeh.2017.03.040>.
- [95] Vangone A, Bonvin AMJJ. “Contacts-based prediction of binding affinity in protein–protein complexes. JULY2015 Elife 2015;4:1–15. <https://doi.org/10.7554/eLife.07454>.
- [96] Xue LC, Rodrigues JP, Kastritis PL, Bonvin AM, Vangone A. PRODIGY: a web server for predicting the binding affinity of protein-protein complexes. *Bioinformatics* 2016;32(23):3676–8. <https://doi.org/10.1093/bioinformatics/btw514>.
- [97] López-Blanco JR, Aliaga JI, Quintana-Ortí ES, Chacón P. IMODS: internal coordinates normal mode analysis server. no. W1 *Nucleic Acids Res* 2014;42. <https://doi.org/10.1093/nar/gku339>.
- [98] López-Blanco JR, Garzón JI, Chacón P. iMod: multipurpose normal mode analysis in internal coordinates. *Bioinformatics* 2011;27(20):2843–50. <https://doi.org/10.1093/bioinformatics/btr497>.
- [99] Kumar N, Sood D, Chandra R. Design and optimization of a subunit vaccine targeting COVID-19 molecular shreds using an immunoinformatics framework. *RSC Adv* 2020;10(59):35856–72. <https://doi.org/10.1039/dora06849g>.
- [100] López-Blanco JR, Aliaga JI, Quintana-Ortí ES, Chacón P. IMODS: internal coordinates normal mode analysis server. *Nucleic Acids Res* 2014;42(W1):1–6. <https://doi.org/10.1093/nar/gku339>.
- [101] Rapin N, Lund O, Bernaschi M, Castiglione F. Computational immunology meets bioinformatics: the use of prediction tools for molecular binding in the simulation of the immune system. *PloS One* 2010;5(4). <https://doi.org/10.1371/journal.pone.0009862>.
- [102] Grote A, et al. JCat: a novel tool to adapt codon usage of a target gene to its potential expression host. *Nucleic Acids Res* 2005;33(SUPPL. 2):526–31. <https://doi.org/10.1093/nar/gki376>.
- [103] Carafa Yda, Brody E, Thermes C. Prediction of rho-independent *Escherichia coli* transcription terminators. A statistical analysis of their RNA stem-loop structures. *J Mol Biol* 1990;216(4):835–58. [https://doi.org/10.1016/S0022-2836\(99\)80005-9](https://doi.org/10.1016/S0022-2836(99)80005-9).
- [104] Ermolaeva MD, Khalak HG, White O, Smith HO, Salzberg SL. Prediction of transcription terminators in bacterial genomes. *J Mol Biol* 2000;301(1):27–33. <https://doi.org/10.1006/jmbi.2000.3836>.
- [105] Solanki V, Tiwari V. Subtractive proteomics to identify novel drug targets and reverse vaccinology for the development of chimeric vaccine against *Acinetobacter baumannii*. *Sci Rep* 2018;8(1):1–19. <https://doi.org/10.1038/s41598-018-26689-7>.
- [106] Sarkar B, Ullah MA, Johora FT, Taniya MA, Araf Y. Immunoinformatics-guided designing of epitope-based subunit vaccines against the SARS Coronavirus-2 (SARS-CoV-2). *Immunobiology* 2020;225(3):151955. <https://doi.org/10.1016/j.imbio.2020.151955>.
- [107] Patronov A, Doytchinova I. T-cell epitope vaccine design by immunoinformatics. *JAN Open Biol.* 2013;3. <https://doi.org/10.1098/rsob.120139>.

- [108] Russi RC, Bourdin E, García MI, Veaute CMI. In silico prediction of T- and B-cell epitopes in PmpD: first step towards to the design of a Chlamydia trachomatis vaccine. *Biomed J* 2018;41(2):109–17. <https://doi.org/10.1016/j.bj.2018.04.007>.
- [109] Tarang S, Kesherwani V, LaTendresse B, Lindgren L, Rocha-Sanchez SM, Weston MD. In silico design of a multivalent vaccine against *Candida albicans*. *Sci Rep* 2020;10(1):1–7. <https://doi.org/10.1038/s41598-020-57906-x>.
- [110] Meza B, Ascencio F, Sierra-Beltrán AP, Torres J, Angulo C. A novel design of a multi-antigenic, multistage and multi-epitope vaccine against *Helicobacter pylori*: an in silico approach. *Infect Genet Evol* 2017;49:309–17. <https://doi.org/10.1016/j.meegid.2017.02.007>.
- [111] Sanchez-trincado JL, Gomez-perosanz M, Reche PA. Review article fundamentals and methods for T- and B-cell epitope prediction, 2017; 2017.
- [112] M. H. V. Van Regenmortel, “Chapter 1 what is a B-cell Epitope ?,” vol. 524, doi: 10.1007/978-1-59745-450-6.
- [113] Misra N, Panda PK, Shah K, Sukla LB, Chaubey P. Population coverage analysis of T-Cell epitopes of *Neisseria meningitidis* serogroup B from Iron acquisition proteins for vaccine design 2011;6(7).
- [114] Sivakumar SM, Safhi MM, Kannadasan M, Sukumaran N. Vaccine adjuvants - current status and prospects on controlled release adjuvanticity. *Saudi Pharmaceut J* 2011;19(4):197–206. <https://doi.org/10.1016/j.jps.2011.06.003>.
- [115] Liu T, et al. Enhancing protein stability with extended disulfide bonds. *Proc. Natl. Acad. Sci. U.S.A* 2016;113(21):5910–5. <https://doi.org/10.1073/pnas.1605363113>.
- [116] Betz SF. Disulfide bonds and the stability of globular proteins. *Protein Sci* 1993;2 (10):1551–8. <https://doi.org/10.1002/pro.5560021002>.